



**Joint Biotechnology Master Program**



Palestine Polytechnic University  
Deanship of Higher Studies and  
Scientific Research



Bethlehem University  
Faculty of Science

**Orf Virus Gene Signatures Associated with Jumping the Host-Species Barrier from Small Ruminants into Humans**

By

**Insaf Hatem Salah Abu Odeh**

In Partial Fulfillment of the Requirements for the Degree

Master of Science

**September 2021**



## Biotechnology Master Program



The undersigned hereby certify that they have read and recommend to the Faculty of Scientific Research and Higher Studies at the Palestine Polytechnic University and the Faculty of Science at Bethlehem University for acceptance a thesis entitled:

**Orf Virus Gene Signatures Associated with Jumping the Host-Species Barrier from Small Ruminants into Humans**

**By**

**Insaf Hatem Salah Abu Odeh**

A thesis submitted in partial fulfillment of the requirements for the degree of Master of Science in biotechnology

Graduate Advisory Committee:

<hr/>	<hr/>
<i>Committee Member (Student's Supervisor)</i>	Date
<i>Dr. Robin Abu Ghazaleh, Palestine Polytechnic University</i>	
<hr/>	<hr/>
<i>Committee Member (Internal Examiner)</i>	Date
<i>Dr. , Palestine Polytechnic University</i>	
<hr/>	<hr/>
<i>Committee Member ( External Examiner)</i>	Date
<i>Dr. ,</i>	

Approved for the Faculties

<hr/>	<hr/>
Dean of Graduate Studies and Scientific Research	Dean of Faculty of Science
Palestine Polytechnic University	Bethlehem University
<hr/>	<hr/>
Date	Date

## ABSTRACT

Orf virus is a member of the parapoxvirus genus that causes contagious ecthyma in the skin of sheep and goats which are its natural hosts, and this sometimes causes high mortality in lambs and kids. Many cases of transmission to humans from infected animals or meat have been reported around the world, but there are no reports of deaths in humans. Understanding the determinants of zoonosis for viruses that are capable of jumping the species barrier is important in order to predict and prevent pandemics that could result from an otherwise unexpected evolutionary shift in a virus that is already capable of infecting humans. Viral determinants of zoonosis have not previously been identified for Orf virus. This study aims to identify potential molecular determinants of Orf virus zoonosis.

A comparative genomic approach was used to screen 17 viral genomes isolated from human and animal hosts for candidate genes that share poor sequence homology between hosts. Multiple sequence alignment and phylogenetic analysis were performed for all candidate genes. As there are only 2 complete genomes for viruses isolated from humans existing in the NCBI database, we gathered local Palestinian Orf virus isolates from 7 human zoonotic events to increase the number of our sequences for candidate gene hypothesis testing.

Phylogenetic analysis of fifteen candidate genes that had been revealed by the comparative genomic approach showed that a distinct human cluster was found in 3 genes. There 12 amino acid substitutions that distinguished the 2 human-derived genomes from the rest (branch IV), One gene was then selected for single gene analysis, and 1 of 5 Palestinian sequences from zoonotic events clustered in branch IV with the 2 genome derived sequences. In addition, 2 sequences from tissue culture adapted Orf viruses were found in the NCBI database, and these also clustered in branch IV, from which it is proposed that there could be determinants within this gene that are associated with host-range preference.

Remarkably, there are 12 novel non-synonymous mutations in one gene that characterize this cluster; four of these substitutions were mapped to a functionally important loop between the  $\beta 7$  and  $\beta 8$  strands and also in  $\beta 1$  and  $\beta 2$  strands, which are binding regions for chemokine, and 5 substitutions are found in sites with unknown functional significance, but where there is absolutely conservation of sequence in natural hosts. To our knowledge, this is the first study to identify molecular determinants that increase the likelihood of Orf virus zoonosis.

## ملخص بالعربية

### دراسة الاختلافات الجزيئية للجينات المرتبطة بانتقال فيروس الإكثمية المعدية (الأورف) من المجترات الصغيرة إلى البشر

"الأورف" هو مرض جلدي تسببه الفيروسات الجدرية، ينتقل للبشر عن طريق التعامل مع الأغنام والماعز أو الذبائح المصابة أو المواد الملوثة. هذا المرض شديد العدوي والخطورة حيث يؤدي غالباً إلى الموت في المضيف الحيواني ولكن لا توجد تقارير عن تسببه بوفيات بين البشر. من المهم أن نفهم المحددات الجزيئية لجميع الفيروسات التي ثبت أنها قادرة على القفز بين الأنواع من أجل التنبؤ بالأوبئة المحتملة والعمل على منعها في المستقبل، حتى لو لم تكن هناك وفيات بين البشر. لم تتم دراسة المحددات الفيروسية لمرض الأورف من قبل لذلك تهدف هذه الدراسة إلى تحديد المحددات الجزيئية المحتملة للإصابة بفيروس أورف حيواني المنشأ.

تم استخدام تحليل مقارنة الجينوم لفحص 17 جينوماً فيروسياً معزولاً من البشر والحيوانات بحثاً عن الجينات المرشحة التي لديها تسلسل مختلف بين المضيفين. يتمثل أحد قيود هذه الدراسة في وجود جينومين كاملين فقط للفيروسات المعزولة عن البشر في قاعدة بيانات NCBI. للتغلب على هذا القيد، قمنا بتجميع عزلات من إصابات بشرية في فلسطين من مصادر مختلفة لزيادة عدد التسلسلات الخاصة بنا لاختبار فرضية الجينات المرشحة.

نتج عن مقارنة بيانات الجينوم لفيروس الأورف 15 جين قد يرتبطون باختلافات تميز الفيروس المعزول من الإنسان عن الحيوانات. ومن ثم تم عمل محاذاة التسلسل وتحليل النشوء والتطور لجميع هذه الجينات، ثلاث جينات أظهرت انفصال الفيروس المعزول من البشر في فرع منفصل عن الحيوانات. تم اختيار جين واحد حيث أظهر 12 طفرة جينية في حين أن الجينات الأخرى لم تظهر هذا العدد، والذي كان مدعوماً جزئياً (1 من 5) من خلال إدراج تسلسلات من العينات الفلسطينية المأخوذة من البشر. بالإضافة إلى ذلك، تم العثور في قاعدة بيانات NCBI على تسلسلين لفيروسات Orf بعد عزلها من أنسجة بعد زراعتها داخل المختبر، وتجمعت هذه التسلسلات في نفس فرع الفيروسات المعزولة من الإنسان، وهذا يدل على إمكانية وجود محددات داخل هذا الجين تحدد تفضيل هذا المضيف.

تم تحديد اثني عشر طفرة جديدة على مستوى الحمض الأميني في جين واحد والتي تميز العزلات الفيروسية من الإنسان وتحديد محددات جزيئية معينة لهذا الفيروس. تم تحديد أربعة من هذه الطفرات في مواقع مهمة وظيفياً في سلسلة  $\beta 1$ ، سلسلة  $\beta 2$  والحلقة الواصلة بين سلسلة  $\beta 7$  وسلسلة  $\beta 8$ . بينما تم تحديد خمسة منها في مواقع محفوظة داخل الجين أهميتها غير الوظيفية غير معروفة.

هذا العمل يوضح ولأول مرة الاختلافات البنائية التي من الممكن أن تبدأ بتفسير تفضيلات فيروس الأورف للأنواع المضيفة والتي يمكن أن تساعد في فهم القفز عبر الأنواع.

## DECLARATION

I declare that the master thesis entitled “Orf Virus Gene Signatures Associated with Jumping the Host-Species Barrier from Small Ruminants into Humans” is my own original work, and thereby certify that unless stated, all work contained within this thesis is my own independent research and has not been submitted for the award of any other degree at any institution, except where due acknowledgment is made in the text.

Name: Insaf Hatem Salah Abu Odeh

Signature: \_\_\_\_\_

Date: \_\_\_\_\_

Copyright ©Insaf Hatem Salah Abu Odeh, 2021  
All rights reserved

## STATEMENT OF PERMISSION TO USE

In presenting this thesis in partial fulfillment of the requirements for the joint master's degree in biotechnology at Palestine Polytechnic University and Bethlehem University, I agree that the library shall make it available to borrowers under rules of the library. Brief quotations from this thesis are allowable without special permission, provided that accurate acknowledgment of the source is made. Permission for extensive quotation from, reproduction, or publication of this thesis may be granted by my main supervisor, or in his absence, by the Dean of Higher Studies when, in the opinion of either, the proposed use of the material is for scholarly purposes. Any copying or use of the material in this thesis for financial gain shall not be allowed without my written permission.

Name: Insaf Hatem Salah Abu Odeh

Signature: \_\_\_\_\_

Date: \_\_\_\_\_

## ACKNOWLEDGMENT

I would like to express my very great appreciation to my supervisor Dr. Robin Abu Ghazaleh for all the critical advice, guidance, support, enthusiastic encouragement and most importantly his patience over the period of my Master.

My grateful thanks are also extended to the faculty staff in the Biotechnology Master Program in Palestine Polytechnic University: Dr. Yaqoub Ashhab, Dr. Rami Arafeh, Dr. Muneef Ayyash, Zaid Al-Tarade and Mr. Ayman Eiadeh for all the support provided.

I would like to thank Hasan Al-Tarade and Asma' Tamimi for the valuable technical support provided in the lab, and for always reminding us about lab safety and to keep us safe and sound. I am still indebted to Yasmin Dweik, Zain Bader and Nour Sharawi who helped to finalize this project.

As well, I thank all the students in the Biotechnology Master Program and virology group who made my time in the lab so enjoyable.

I would also like to thank Dr. Jihad El-Ebrahimi, Dr. Mohammad Manassra, Abdullah Alheeh and Hasan Al-Tarade for providing the Orf virus samples, which were used in this study.

Lastly, there are no words that I can say to convey my appreciation for my parents for their continuous support and encouragement throughout my study. All these successes would have been impossible without them and I could not have become the person I am today without them in my life.

## List of abbreviations

<b>BLAST</b>	Basic Local Alignment Search Tool
<b>Bp</b>	Base pair
<b>BPSV</b>	Bovine papular stomatitis virus
<b>CEV</b>	Cell-associated extracellular enveloped virion
<b>CBP</b>	Chemokine Binding protein
<b>CD-hit</b>	Cluster Database at High Identity with Tolerance
<b>C, CC, CXC, CX3C</b>	chemokine classes, also known as $\gamma$ , $\beta$ , $\alpha$ , and $\delta$ (respectively)
<b>DNA</b>	Deoxyribonucleic acid
<b>dNTPs</b>	Deoxynucleotides
<b>EEV</b>	Extracellular Enveloped Virion
<b>ELISA</b>	Enzyme linked immunosorbent assay
<b>EV</b>	Enveloped Virion
<b>EM</b>	Electron microscopy
<b>FMD</b>	Foot and Mouth Disease
<b>G</b>	Gravitational force
<b>GAGs</b>	Glycosaminoglycan
<b>GFF3</b>	General Feature Format version 3
<b>GIF</b>	IL-2 inhibitory factor
<b>GM-CSF</b>	Granulocyte-macrophage colony-stimulating factor
<b>GPCR</b>	G protein–coupled receptor
<b>IEV</b>	Intracellular enveloped virion
<b>IFN</b>	Interferon
<b>IL-10</b>	Interleukin-10
<b>IL-2</b>	Interleukin-2
<b>IMV</b>	Intracellular Mature Virion
<b>ITR</b>	Inverted terminal repeats
<b>Kbp</b>	Kilobase pair
<b>KDa</b>	kilo Dalton
<b>LBs</b>	lateral bodies
<b>MAFFT</b>	Multiple Alignment using Fast Fourier Transform
<b>MEGA</b>	Molecular Evolution Genetic Analysis
<b>MCL</b>	Markov Cluster Algorithm
<b>mRNA</b>	Messenger ribonucleic acid



<b>MV</b>	Mature Virion
<b>Mg</b>	Microgram
<b>ml</b>	Microlitre
<b>mM</b>	Millimolar
<b>μM</b>	Micromolar
<b>MW</b>	Molecular weight
<b>NCBI</b>	National Center for Biotechnology Information
<b>ORFV</b>	Orf virus
<b>PBS</b>	Phosphate-buffered saline
<b>PCPV</b>	Pseudocowpoxvirus
<b>PCR</b>	Polymerase chain reaction
<b>PKR</b>	dsRNA dependent Protein kinase-R
<b>Pmol</b>	picomoles
<b>PPU</b>	Palestine Polytechnic University
<b>PPV</b>	Parapoxvirus
<b>PVNZ</b>	Parapoxvirus of red deer in New Zealand
<b>RFLP</b>	Restricted fragment length polymorphism
<b>ROARY</b>	Rapid large-scale prokaryote pan genome analysis
<b>RPM</b>	Revolution per minute
<b>T.C.</b>	Tissue Culture
<b>TFN</b>	Tumor Necrosis Factor
<b>Tm</b>	Melting temperature
<b>TBE</b>	Tris-borate-EDTA
<b>UV</b>	Ultraviolet
<b>vCBPs</b>	Viral Chemokine Binding Proteins
<b>VEGFs</b>	Vascular endothelial growth factors
<b>VIR</b>	Virulence interferon resistance
<b>VV</b>	Vaccinia virus
<b>WV</b>	Wrapped virion
<b>w/v</b>	Weight to volume

## List of Figures

Figure 1.1: Electron micrograph of negatively stained ORFV. ....	2
Figure 1.2: The structure of Mature and enveloped virion in Parapoxviruses.....	3
Figure 1.3: The structure of the genome of ORFV strain . ....	4
Figure 1.4: Clinical signs of ORFV infection in sheep.....	6
Figure 1.5: Clinical signs of ORFV infection in human .....	7
Figure 1.6: Diagrammatical representation of select poxvirus-encoded immunomodulatory proteins .....	10
Figure 1.7: Viral chemokine binding proteins (vCBP) interfere with chemokine .....	<b>Error! Bookmark not defined.</b>
Figure 3.1 Summary of the comparative genomic analysis and downstream protocol applied to ORFV genomes for the selection of variable gene candidates. ....	12
Figure 3.2: Screenshot of input preparation step showed the script for converting file format from genbank into GFF3.....	14
Figure 3.3: Screenshots of the ROARY selected steps. ....	15
Figure 3.4: A flowchart of the steps of ROARY application.....	16
Figure 4.1: Summary of the resulted genes in each step of the pipeline for molecular marker candidates' criteria .....	25
Figure 4.2: Phylogenetic analysis based on dUTPase nucleotide sequences.....	27
Figure 4.3: Phylogenetic analysis based on EEV glycoprotein nucleotide sequences.....	28
Figure 4.4: Phylogenetic analysis based on CBP nucleotide sequences .....	29
Figure 4.5: A representative Agarose gel electrophoresis of 1030bp of the full length CBP gene .....	30
Figure 4.6: Phylogenetic analysis based on CBP amino acid sequences .....	33
Figure 4.7: Species specific markers for CBP at the amino acid level for 12 sites.....	34
Figure 4.8: Clinical presentations of Orf lesions in the 2 brothers. ....	36
Figure 4.9: Clinical presentations of orf lesion stages in case 6 .....	38
Figure 4.10: A representative Agarose gel electrophoresis of 1005bp of the full length F1L gene of ORFV amplified by PCR .....	39
Figure 4.11: Phylogenetic analysis based on F1L nucleotide sequences distinguishing the viral strain in the three infections. ....	40
Figure S.1: Phylogenetic analysis based on ORF001 nucleotide sequences.....	55
Figure S.2: Phylogenetic analysis based on ORF005 nucleotide sequences.....	56
Figure S.3: Phylogenetic analysis based on ORF012 nucleotide sequences.....	57
Figure S.4: Phylogenetic analysis based on ORF017 nucleotide sequences.....	58
Figure S.5: Phylogenetic analysis based on ORF 046 nucleotide sequences.....	58
Figure S.6: Phylogenetic analysis based on ORF056 nucleotide sequences.....	59
Figure S.7: Phylogenetic analysis based on ORF059 nucleotide sequences.....	60
Figure S.8: Phylogenetic analysis based on ORF080 nucleotide sequences.....	61
Figure S.9: Phylogenetic analysis based on ORF088 nucleotide sequences.....	62
Figure S.10: Phylogenetic analysis based on ORF116 nucleotide sequences.....	62
Figure S.11: Phylogenetic analysis based on ORF120 nucleotide sequences.....	63

Figure S.12: Phylogenetic analysis based on ORF132 nucleotide sequences.....	64
Figure S.13: Divergence of F1L gene of ORFV in the 5'-terminal region.....	65

## List of Tables

Table 3.1: GenBank accession number for complete genome sequences of ORFV.....	13
Table 3.2: Palestinian human Orf virus isolates from different regions in West Bank.....	17
Table 3.3: Description of primers for PCR that target the CBP and F1L genes of Orf virus. ....	19
Table 3.4: GenBank accession number of Orf virus isolates which have the full length of CBP gene with host, country and year of collection. ....	22
Table 4.1: Potential candidate genes list.....	26

## Table of Contents

<b>CHAPTER (1) .....</b>	<b>1</b>
<b>1. INTRODUCTION.....</b>	<b>1</b>
<b>1.1. Orf virus overview .....</b>	<b>1</b>
<b>1.2. Orf virus structure.....</b>	<b>1</b>
<b>1.3. Orf virus genome.....</b>	<b>3</b>
<b>1.4. Orf virus replication cycle.....</b>	<b>4</b>
<b>1.5. Orf virus host range.....</b>	<b>4</b>
<b>1.6. Orf virus transmission.....</b>	<b>5</b>
<b>1.7. Clinical Symptoms and Lesions.....</b>	<b>6</b>
<b>1.8. Orf virus diagnosis and immunity.....</b>	<b>8</b>
<b>1.9. Prevention and control .....</b>	<b>8</b>
<b>1.10. Viral Immune evasion.....</b>	<b>9</b>
<b>CHAPTER (2) .....</b>	<b>11</b>
<b>2. OBJECTIVES .....</b>	<b>11</b>

<b>CHAPTER (3)</b> .....	<b>12</b>
<b>3. MATERIALS AND METHODS</b> .....	<b>12</b>
<b>3.1. Comparative genome Analysis</b> .....	<b>12</b>
3.1.1. Data retrieval.....	13
3.1.2. Input preparation.....	14
3.1.3. All against all comparison of open reading frames from 17 NCBI genomes using ROARY.....	14
3.1.4. Multiple sequence alignment and phylogenetic analyses for the selected variable genes .....	16
<b>3.2. Virus isolation and single gene analysis</b> .....	<b>17</b>
3.2.1. Sample collection and summary of ORFV isolates .....	17
3.2.2. ORFV DNA extraction .....	18
3.2.3. Primer design .....	18
3.2.4. Polymerase Chain Reaction (PCR) reaction conditions .....	19
3.2.5. Electrophoresis.....	20
3.2.6. Purification and sequencing of PCR products .....	20
3.2.7. DNA sequencing:.....	21
3.2.8. Multiple sequence alignment and phylogenetic analysis.....	22
3.2.9. Sequence logo generation .....	24
<b>CHAPTER (4)</b> .....	<b>25</b>
<b>4. RESULTS</b> .....	<b>25</b>
<b>4.1 Comparative genome analysis</b> .....	<b>26</b>
<b>4.2. Multiple sequence alignment and phylogenetic tree of candidate genes</b> .....	<b>26</b>
<b>4.3. CBP gene based analysis</b> .....	<b>29</b>
4.3.1. Amplification of the CBP gene from local human ORFV isolates.....	29
4.3.2. Phylogenetic analysis of the full length CBP gene including Palestinian isolates .....	30
4.3.3. Species specific amino acid variations in the CBP protein.....	33
<b>4.4. Case presentation</b> .....	<b>35</b>
4.4.1. Recurrent zoonotic infection from the same Palestinian farm.....	35
4.4.2. Other zoonotic cases .....	37
<b>4.5. F1L gene based analysis</b> .....	<b>38</b>
4.5.1. Amplification of the F1L gene from ORFV isolates in the three outbreaks.....	38
4.5.2. Phylogenetic analysis of ORFV based on the full length F1L gene .....	39
<b>CHAPTER (5)</b> .....	<b>41</b>

<b>5. DISCUSSION .....</b>	<b>41</b>
<b>CHAPTER (6) .....</b>	<b>45</b>
<b>6. CONCLUSION .....</b>	<b>45</b>
<b>REFERENCES.....</b>	<b>46</b>
<b>SUPPLEMENTARY DATA .....</b>	<b>55</b>

## CHAPTER (1)

### 1. INTRODUCTION

#### 1.1. Orf virus overview

Orf virus is a member of the *Poxviridae* family of large DNA viruses, which is divided into two subfamilies: the *Entomopoxvirinae*, members of which infect invertebrates and the *Chordopoxvirinae*, members of which infect vertebrates. *Chordopoxvirinae* are divided among ten genera: *Avipoxviruses*, *Molluscipoxviruses*, *Parapoxviruses*, *Orthopoxviruses*, *Yatapoxviruses*, *Leporipoxviruses*, *Capripoxviruses*, *Cervidpoxviruses*, *Crocodylidpoxvirus* and *Suipoxviruses* (A. Bratkea, McLysaghta, 2013; Barrett & McFadden, 2008).

*Parapoxviruses* (PPVs) represent one of the ten genera within the Chordopoxvirinae subfamily, and comprise Orf virus (ORFV), Bovine papular stomatitis virus (BPSV), Pseudocowpox virus (PCPV), and PPVs of red deer in New Zealand (Fleming & Mercer, 2007). ORFV causes "contagious ecthyma" synonymously known as Orf, contagious pustular dermatitis, infectious labial dermatitis, scabby mouth, or sore mouth, (Fleming & Mercer, 2007).

#### 1.2. Orf virus structure

The Orf virion particle is ovoid-shaped with a spiral tubule wrapped around the outer surface in a criss-cross pattern, which is a feature of parapoxviruses. It is about ~260 nm long and ~160 nm wide, and is relatively smaller than other members of the Poxviridae family (**Figure 1.1**) (Fleming & Mercer, 2007; Spehner et al., 2004; J. L. Tan et al., 2009).

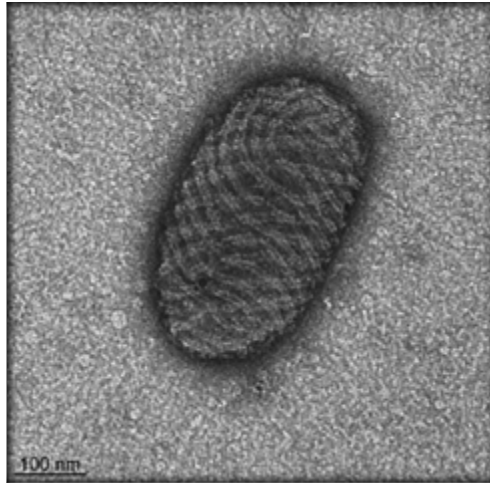


**Figure 1.1: Electron micrograph of negatively stained ORFV.** The ovoid appearance of the virion surface with its crisscross patterned tubule-like structure is evident (Spehner et al., 2004).

The virion particle can exist in three forms: the first is the Mature Virion (MV, also called Intracellular Mature Virion, IMV), which is formed within a virally induced cytoplasmic factory. MV represents the majority of infectious progeny and is surrounded by a single lipid bilayer membrane as it shown in **Figure 1.2**. When MVs leave the factory and are wrapped with a second lipid bilayer membrane obtained from the trans-Golgi or endosomes they are referred to as Wrapped Virions (WVs), which is the second form. WVs travel to the cell surface via microtubules where the outer membrane of the additional layers fuses with the plasma membrane to comprise the third form, the extracellular virion (EV), which is either released outside the cell by exocytosis (EEV, extracellular enveloped virion) or remains attached to the cell surface to form the fused virion (CEV, cell-associated extracellular enveloped virion). These virions are infectious and the diversity in their surface structure affects the properties and functions of each type of particle (Fleming & Mercer, 2007; Ichihashi, 1996; Smith et al., 2002).

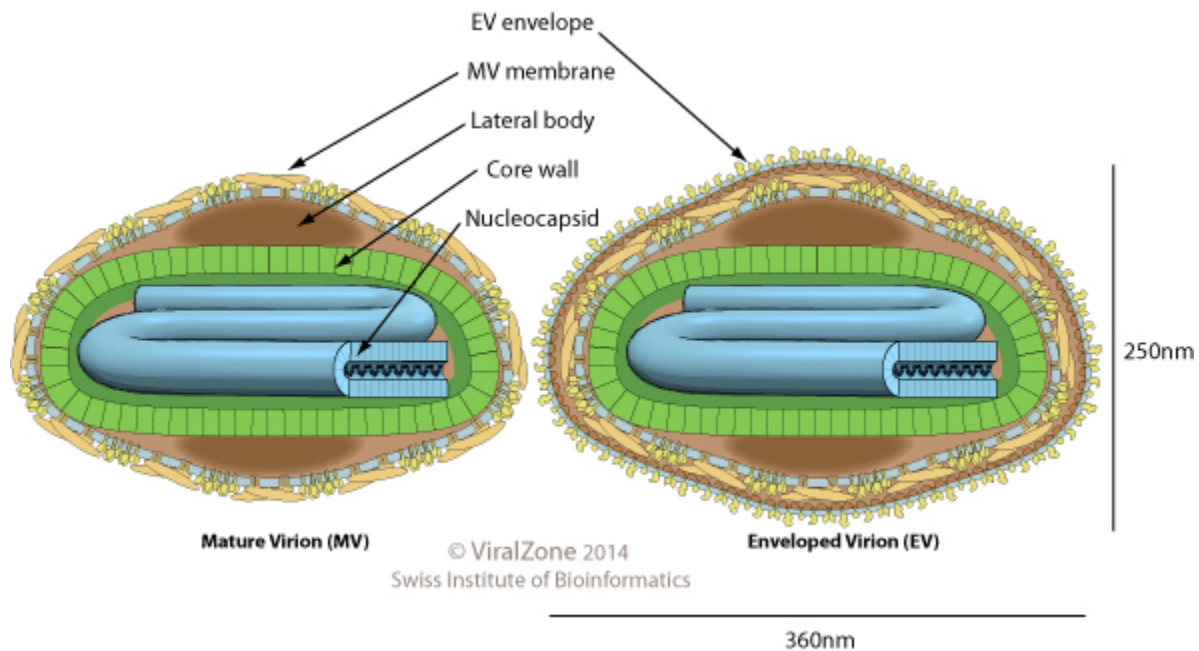


**Figure 1.2: The structure of Mature and enveloped virion in Parapoxviruses.** Lateral bodies (LBs) are delivery containers for viral enzymes, MV mature virion, EV enveloped virion.

### 1.3. Orf virus genome

The genome of ORFV is linear double- stranded DNA with covalently closed hairpin termini, and is about 138-140 kbp. The G+C composition of ORFV is high (around 64%) (Delhon et al., 2004). The virus encodes 132 putative genes that include 89 highly conserved genes that are found at the central region of the genome (the core) required for morphogenesis, structure and basic replication mechanisms and some variable genes located on both strands in the terminal ends of the genome which are called inverted terminal repeats (ITR), that although not essential for growth are important in determining virulence, host range and interaction with or evasion of the host's immune system as it shown in **Figure 1.3** (Fleming et al., 2015).



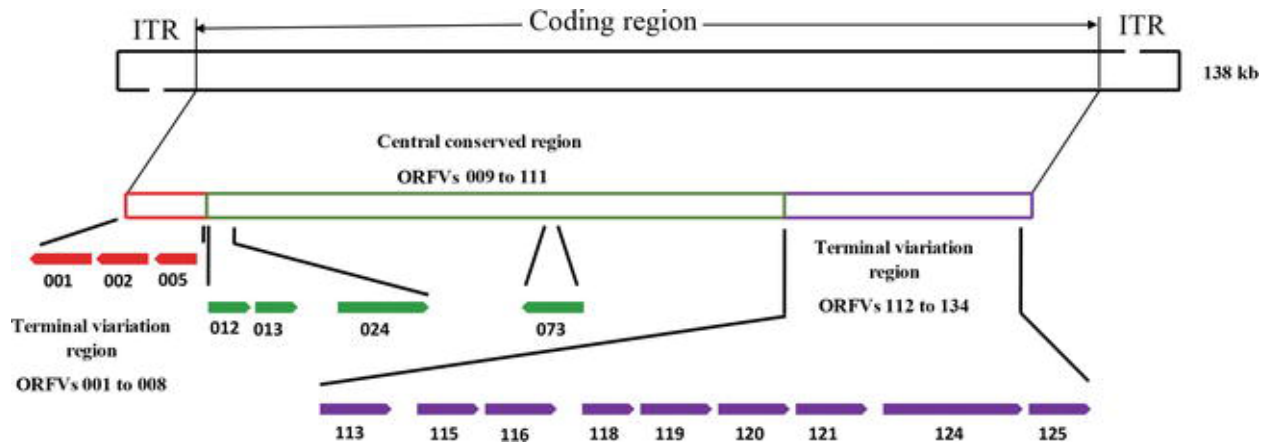


**Figure 1.3:**The structure of the genome ORFV strain (Wang & Luo, 2018).

## 1.4. Orf virus replication cycle

DNA viruses usually use host cell proteins and enzymes to replicate their genomes in the nucleus. In contrast, ORFV replication takes place in the cytoplasm of host cells, and hence the virus encodes all enzymes required for transcription and replication of its genome (Moss, 2012). Attachment is the first step in viral replication, and the binding of ORFV to the host cell is mediated by cell-surface glycosaminoglycans (GAGs), followed by endocytosis of the virus, and subsequent release of the viral core into the cytoplasm. The transcription of the ORFV genome is regulated temporally and hence viral genes can be divided into early genes and delayed intermediate genes during initiation of DNA replication, and late genes after initiation of DNA replication.

In the early phase, the virus replicates early genes by its viral RNA polymerase within minutes after infection that mediate fully uncoating of the core and required for intermediate gene transcription. The intermediate phase results in production of transcription factors needed to mediate late gene expression. Late genes are expressed to produce the structural proteins that required for morphogenesis. Following the assembly of the virus particles, the virions are released by exocytosis and by budding or cell lysis (James, 2017; Moss, 2013; Schmid et al., 2014).

## 1.5. Orf virus host range

ORFV is a highly contagious disease that mainly affects sheep and goats, while other animals including camels, reindeer, Sichuan takin, deer, alpaca, cleft horn antelope, wapiti, Japanese

sero, blackbuck, cats and seal squirrels can be affected (Azwai et al., 1995; Fairley et al., 2008; Frandsen et al., 2011; Guo et al., 2004; R. Kumar et al., 2015; Kummeneje & Krogsrud, 1979; Robinson & Mercer, 1995; Sharma et al., 2016; Thomas et al., 2003; Tryland et al., 2005). The virus is zoonotic and people who have direct contact with infected animals can also be infected such as veterinarians, farmers, abattoir workers, wool shearers, shepherds and nonprofessional people such as children and housewives of farmers, and Muslims who slaughter sacrifices on Eid al-Adha, and visitors to zoos (A. Bratke, McLysaghta et al., 2019; Andreani et al., 2019; Nougairede et al., 2013).

### **1.6. Orf virus transmission**

ORFV spreads through direct and indirect contact. However, the virus cannot penetrate the normal unbroken skin; small abrasions are sufficient to allow infection. In indirect transmission, infected animals shed the virus through scab materials to the environment. Then, the contaminated environment (grass, ear tag or oral gavage tube) becomes the source of infection for susceptible animals. (Bala et al., 2019; R. Kumar et al., 2015; Zeedan, 2015). The virus particles in the dried scabs may survive for 8 months or more and contaminate the environment (Manley, 1934; S. T. Tan et al., 1991).

ORFV can be transmitted to humans by close and direct physical contact with infected animals or contaminated objects (Andreani et al., 2019; Tedla et al., 2018). The disease was reported in humans for the first time in 1934 (Newsom & Cross, 1934). Human to human transmission events are rare, but six cases have been recorded in the literature : a case of transmission from infected patient to nurse during dressing change (Westphal, 1973), two cases of transmission between infected mother and child and one case from father to daughter (Kennedy & Lyell, 1984; Rajkomar et al., 2016; Turk et al., 2013), and a case of transmission from a farmer's husband to his wife, and a case of transmission from infected wife to her husband (Bouscarat & Descamps, 2017; Stewart, 1983). It is possible for the ORFV to spread by autoinoculation. There have been three reported cases that developed lesions on their fingers and was later found on different body parts include perianal, genitals and face (Duchateau et al., 2014; Kennedy & Lyell, 1984; Stead et al., 1992). The first outbreak of a nosocomial ORFV infection was reported in a hospital burn unit in Gaziantep, Turkey in 2012 where 13 patients became infected (Midilli et al., 2013).

### 1.7. Clinical Symptoms and Lesions

Clinically, in sheep and goat the ORFV produce proliferative lesions appear 6 to 7 days after infection on the skin, lips and oral mucosa as well as around the nostrils. It can be also seen in the buccal cavity, respiratory tract, esophagus, stomach and intestine of the infected animal (**Figure 1.4**). Complete healing of skin lesions may take up to 6-8 weeks, but in some cases severe proliferative dermatitis develops and death is common in young lambs (Fleming & Mercer, 2007; Li et al., 2015; Spyrou & Valiakos, 2015).

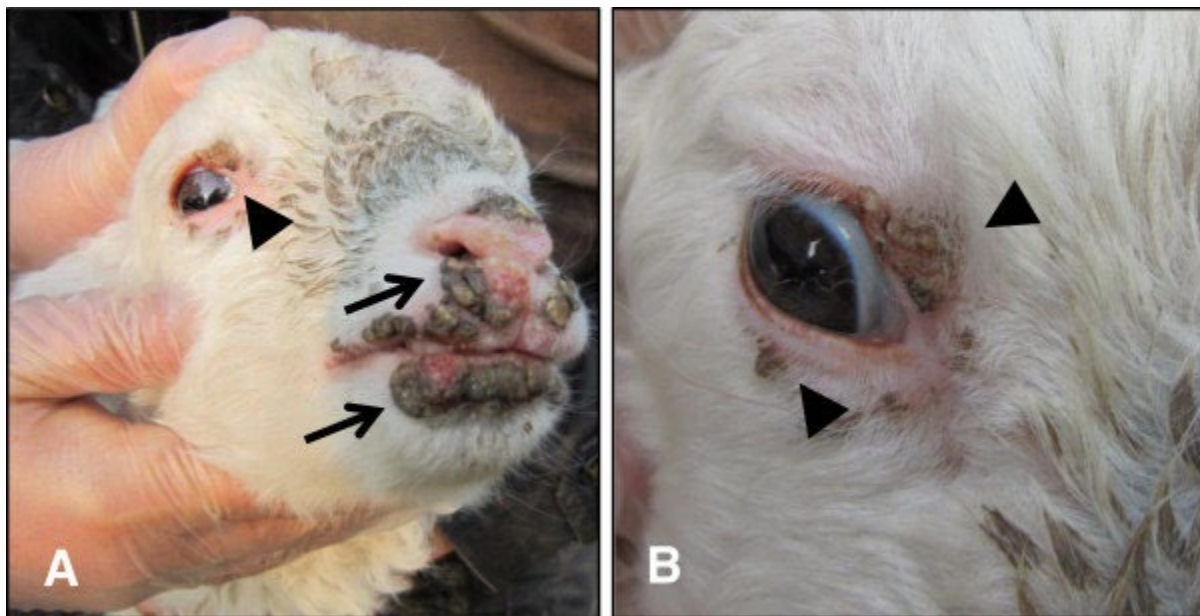


**Figure 1.4: Clinical signs of ORFV infection in sheep.** A. Proliferative lesions on the skin of mouth, lips, muzzle and nostrils (arrows). B. lesions on the eyelids (arrowheads) (Li et al., 2012).

The disease in humans is usually characterized by the development of localized lesions on fingers, hands and forearms (**Figure 1.5 A and B**), but it can also be found in face, nose, scalp, axilla, buttocks and in the *genital* organs (Bouscarat & Descamps, 2017; Turk et al., 2013). Additional clinical manifestations such as mild fever, malaise, and local swelling of lymph nodes may occur (Bergqvist et al., 2017; Spyrou & Valiakos, 2015).

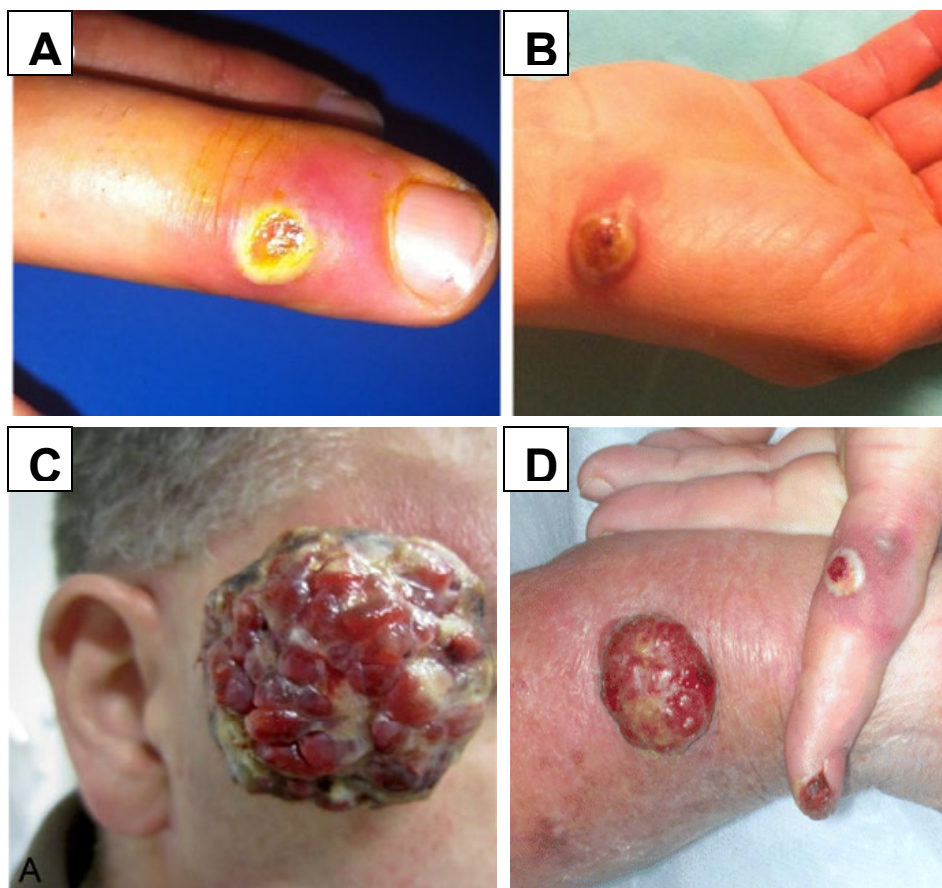


**Figure 1.5: Clinical signs of ORFV infection in human.** (A,B). Cutaneous lesions on hand (Nougairede et al., 2013). **C.** Initial presentation of the temporal giant ORFV lesion on face (Rørdam et al., 2013). **D.** Vascular noduloulcerative Orf lesions on hand (Lederman et al., 2007).

The human lesions pass through six clinical stages before healing, each lasts about one week. Briefly, after 3 to 5 days of incubation, the lesions appear as erythematous macules and then transform into papules, later the lesions progress to weeping proliferative nodules and pustules. Finally, lesion dry, flatten and scabs develop. After a scab appears, uncomplicated lesions usually resolve on their own without scarring (Bergqvist et al., 2017; Muhsen et al., 2019; Nougairede et al., 2013; Uzel et al., 2005). In immunocompromised individuals, highly vascularised tumor-like lesions of the skin have been reported called giant Orf (**Figure 1.5.C and D**) (Ballanger et al., 2006; S. T. Tan et al., 1991).

## **1.8. Orf virus diagnosis and immunity**

Generally, the diagnosis of ORFV is based on the clinical symptoms and lesions in the affected animals. However, the disease may need to be differentially diagnosed from other diseases (FMD, capripox and bluetongue), which produce lesions similar to ORFV. In humans, diagnosis can be made based on the clinical signs, and it can be easy if there is any historical contact with animals. Misdiagnosis of orf can lead to several complications in some people, including immunocompromised individuals and children. Several diagnostic methods are available for the detection of ORFV. Various tests such as cell culture isolation, polymerase chain reaction (PCR) assays, real-time PCR, electron microscopy (EM), immunohistochemistry, ELISA, restricted fragment length polymorphism (RFLP), and demonstration of neutralizing antibodies are employed for diagnosis of ORFV (Ahanger et al., 2018; Guo et al., 2004; Hosamani et al., 2009; Zeedan, 2015).

The hosts which recover from the disease will commonly develop a short term immune memory that spans 6 to 8 months (Gill et al., 1990), and reinfection of the same host may occur as immunity wanes, but with milder symptoms and quicker healing than the first encounter with the virus (D. Haig, 2006; D. M. K. Haig et al., 1997).

## **1.9. Prevention and control**

There's no precise treatment available for ORFV infection. It is recommended to apply externally topical antiseptic and analgesics on proliferating lesions which will help to improve the healing process and antibiotics to prevent secondary bacterial infection. Human treatment of Orf is often the same as affected animal treatment using topical cidofovir or imiquimod and is focused on secondary infection, along with the use of cryotherapy and surgical excision in the complicated cases (Hosamani et al., 2009; Lederman et al., 2007; Nandi et al., 2011).

To curtail the spread of ORFV disease, infected animals should be isolated in a separate place from susceptible ones, especially young and pregnant animals. Personal hygiene of individuals who are handling or having any other contact with animals is of importance in lowering transmission of ORFV (Bergqvist et al., 2017; Spyrou & Valiakos, 2015).

Vaccination against ORFV in animals can be accomplished using attenuated live ORFV which produces immunity lasting for 4 to 6 months and it's effective in reducing the severity of the

disease and economic losses in the farm if given to ewes in the early stages of gestation. The use of living virus vaccine could be the source of the outbreak in endemic countries (Bala et al., 2018; Nandi et al., 2011). In humans, there is no efficient vaccine to prevent ORFV (Bergqvist et al., 2017).

### **1.10. Viral Immune evasion**

Many organisms have complex defense mechanisms against viral infections that can recognize these invasive pathogens and limit their ability to replicate successfully. The intricacy of virus propagation in host cells has originated from the co-evolution of viruses alongside their hosts. Where a host evolves new mechanisms to protect against viral infection, the virus develops new methods of evasion (Sharp & Simmonds, 2011). There are a range of immune evasion strategies used by viruses, with different families of viruses often utilizing distinct evasion techniques, including antigenic drift, latency, and immune modulation (Alcami & Koszinowski, 2000).

Large DNA viruses, including poxvirus and herpes virus families have developed a range of methods to inhibit the inflammatory response of the host. These viruses produce protein homologues for the purpose of immune evasion called virulence factors secreted during the early stages of infection (Lalani & McFadden, 1997). This secretion of homologous proteins observed by viruses is a result from the virus previously capturing host genes, or even evolving its own (Alcami & Koszinowski, 2000; Felix et al., 2016). Poxviruses encode multiple classes of immunomodulatory proteins (**Figure 1.6**) to mimics, either structurally or functionally, host proteins involved in typical immune regulation and block different aspects of the immune response to which the virus is exposed (Engel & Angulo, 2012; Lalani & McFadden, 1997). These proteins include production of viral inhibitors of interferons and IL-18, homologues of host cytokines, chemokines, tumor necrosis factor (TNF) and interleukin-1 $\beta$  (IL-1 $\beta$ ) homologues of their receptors, inflammation modulatory protein; vascular endothelial growth factor (VEGF) and granulocyte-macrophage colony-stimulating factor/IL-2 factor (GIF) (Johnston & McFadden, 2003; Moss & Shisler, 2001).



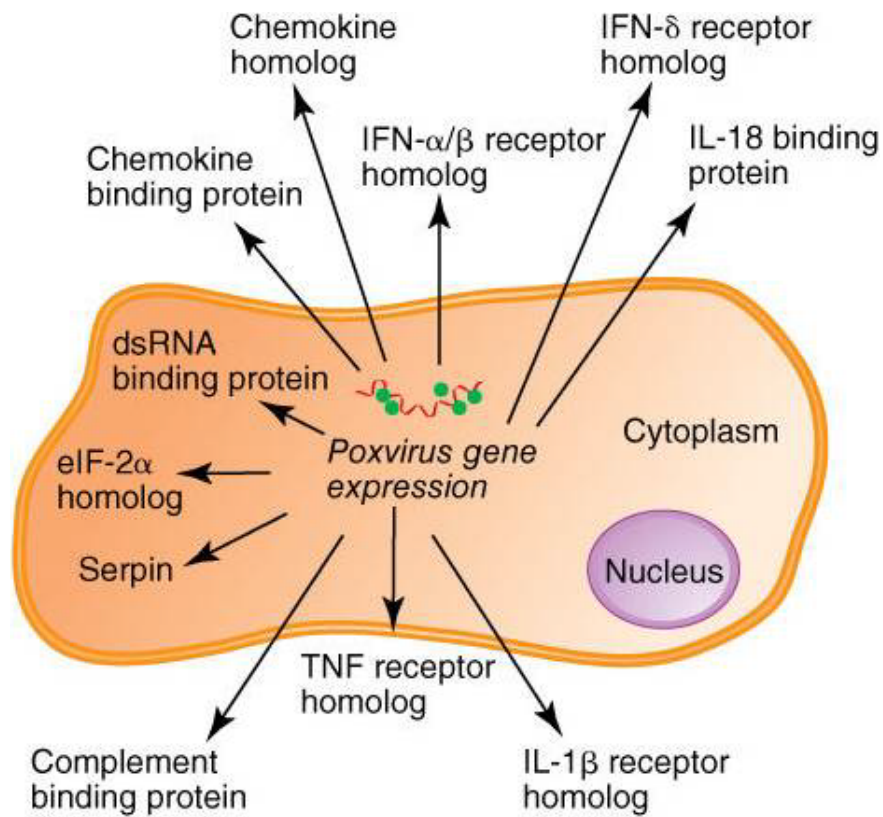


**Figure 1.6: Diagrammatical representation of select poxvirus-encoded immunomodulatory proteins** (Moss & Shisler, 2001).

## **CHAPTER (2)**

### **2. Objectives**

1. To combine comparative genome and phylogenetic analysis approaches to identify potential molecular determinants of ORFV zoonosis.
2. To expand the number of human- derived ORFV samples.
3. To characterize zoonoses and molecular epidemiology in a unusual zoonotic episode on a Palestinian farm that recurred after an interval of four years.



## CHAPTER (3)

### 3. MATERIALS AND METHODS

#### 3.1. Comparative genome Analysis

To identify ORFV genes where evolution may have acted to produce variants with a selective advantage for human hosts, all-against-all sequence alignments among ORFV genomes was performed using a tool called ROARY (rapid large-scale prokaryote pan genome analysis), which provides a list of genes that have low or no sequence homology with other inputs and are found in a small subset of genomes.

The workflow is summarized in **Figure 3.1**. Briefly, in the first phase, the retrieved genomes were analyzed to extract variable genes among all 17 available genomes of ORFV strains. Following the cluster analysis, variable genes among human derived ORFV isolates were selected for further analyzed in this research. In the last stage, multiple sequence alignments and phylogenetic analyses were performed to identify likely molecular determinant(s) of zoonosis.

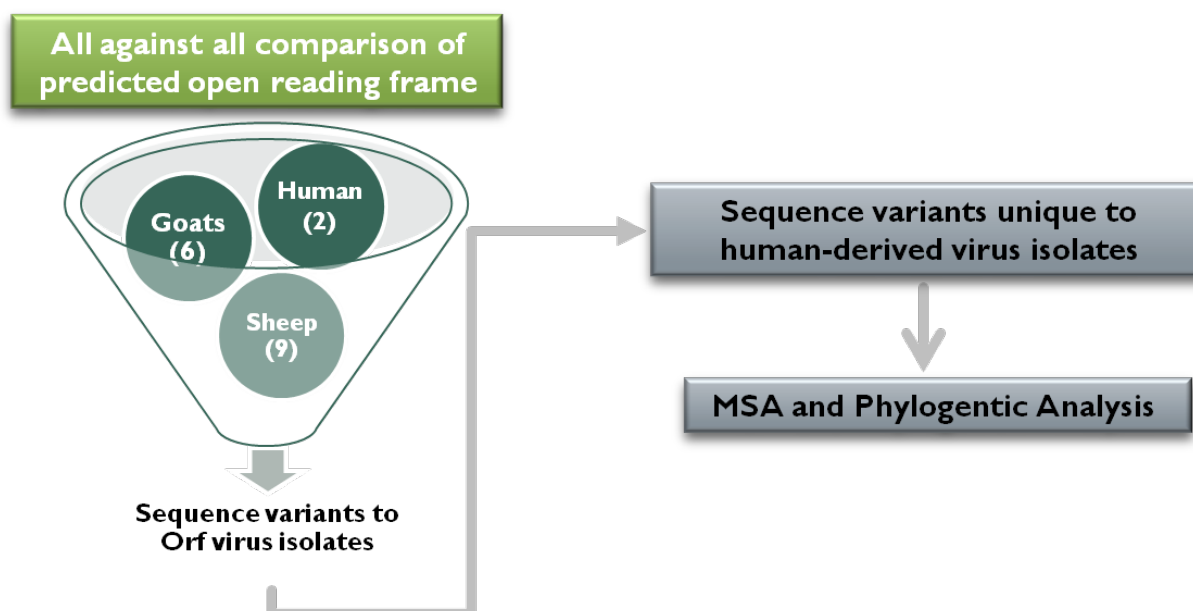


**Figure 3.1** Summary of the comparative genomic analysis and downstream protocol applied to ORFV genomes for the selection of variable gene candidates.

### 3.1.1. Data retrieval

The full GenBank format sequences for all available genome sequences of ORFV (17 ORFV genomes isolated from human and animal hosts) were downloaded from the GenBank - NCBI (as of July 2020). Strain names, with host, country, and year of the collection are shown in **Table 3.1**.

**Table 3.1: GenBank accession number for complete genome sequences of ORFV**

	Accession number	Strain	Host	Country	Year
1	KF837136.1	B029	Human	Germany	1996
2	HM133903.1	D1701	Sheep	Germany	2010
3	KP010354.1	GO	Goat	China	2012
4	KP010356.1	SJ1	Goat	China	2012
5	KP010353.1	YX	Goat	China	2012
6	KP010355.1	NP	Goat	China	2012
7	KF234407.1	NA/11	Sheep	China	2011
8	MN648218.1	GZ18	Sheep	China	2018
9	MN648219.1	CL18	Sheep	China	2018
10	MG674916.2	NA17	Goat	China	2019
11	MG712417.1	SY17	Sheep	China	2016
12	KY053526.1	OV-H3/12	Sheep	China	2012
13	DQ184476.1	NZ2	Sheep	New Zealand	2005
14	AY386263.1	OV-IA82	Lamb	USA	2004
15	AY386264.1	OV-SA00	Ovine	USA	2003
16	MN454854.1	TVL	Ovine	USA	2019

17	LR594616.1	IHUMI-1	Human	France	2017
----	------------	---------	-------	--------	------

### 3.1.2. Input preparation

To run ROARY, input files should be in GFF3 format (General Feature Format version 3) containing both annotation and nucleotide sequence at the end of the file. However, NCBI provides GFF3 files for ORFV that only include annotation, which cannot be used by ROARY (Page et al., 2015). Therefore, the complete genomes of ORFV were first downloaded in standard GenBank format; the format contains the annotation plus nucleotide sequence, which were then converted to GFF3 by using the Bio::Perl script *bp\_genbank2gff3.pl* from (<http://sanger-pathogens.github.io/Roary/>), as shown in **Figure 3.2**.

```
biolinux-ppu@biolinuxppu[Orf Virus] bp_genbank2gff3 -r AY386264.1.gb -out stdout >AY386264.1.gff3
biolinux-ppu@biolinuxppu[Orf Virus] bp_genbank2gff3 -r AY386263.1.gb -out stdout >AY386263.1.gff3
biolinux-ppu@biolinuxppu[Orf Virus] bp_genbank2gff3 -r DQ184476.1.gb -out stdout >DQ184476.1.gff3
biolinux-ppu@biolinuxppu[Orf Virus] bp_genbank2gff3 -r HM133903.1.gb -out stdout >HM133903.1.gff3
biolinux-ppu@biolinuxppu[Orf Virus] bp_genbank2gff3 -r KF234407.1.gb -out stdout >KF234407.1.gff3
biolinux-ppu@biolinuxppu[Orf Virus] bp_genbank2gff3 -r KF837136.1.gb -out stdout >KF837136.1.gff3
biolinux-ppu@biolinuxppu[Orf Virus] bp_genbank2gff3 -r KP010353.1.gb -out stdout >KP010353.1.gff3
biolinux-ppu@biolinuxppu[Orf Virus] bp_genbank2gff3 -r KP010354.1.gb -out stdout >KP010354.1.gff3
biolinux-ppu@biolinuxppu[Orf Virus] bp_genbank2gff3 -r KP010355.1.gb -out stdout >KP010355.1.gff3
biolinux-ppu@biolinuxppu[Orf Virus] bp_genbank2gff3 -r KP010356.1.gb -out stdout >KP010356.1.gff3
biolinux-ppu@biolinuxppu[Orf Virus] bp_genbank2gff3 -r KY053526.1.gb -out stdout >KY053526.1.gff3
biolinux-ppu@biolinuxppu[Orf Virus] bp_genbank2gff3 -r LR594616.1.gb -out stdout >LR594616.1.gff3
biolinux-ppu@biolinuxppu[Orf Virus] bp_genbank2gff3 -r MG674916.2.gb -out stdout >MG674916.2.gff3
biolinux-ppu@biolinuxppu[Orf Virus] bp_genbank2gff3 -r MG12417.1.gb -out stdout >MG12417.1.gff3
biolinux-ppu@biolinuxppu[Orf Virus] bp_genbank2gff3 -r MN331655.1.gb -out stdout >MN331655.1.gff3
biolinux-ppu@biolinuxppu[Orf Virus] bp_genbank2gff3 -r MN389453.1.gb -out stdout >MN389453.1.gff3
biolinux-ppu@biolinuxppu[Orf Virus] bp_genbank2gff3 -r MN454854.1.gb -out stdout >MN454854.1.gff3
```

**Figure 3.2:** Screenshot of input preparation step showed the script for converting file format from genebank into GFF3.

### 3.1.3. All against all comparison of open reading frames from 17 NCBI genomes using ROARY

The comparative genomic analysis was performed using ROARY with its default parameters except for the translation table value, which in this study was set to 1 instead of 11, as 11 is the

genetic code used by bacteria, archaea and chloroplast proteins while for virus data, it is recommended to set the translation table to 1, which is the standard genetic code (Elzanowski et al., n.d). The analysis for 17 threads was generated with ROARY script option: Roary -e --mafft -p 17 \*.gff (<http://sanger-pathogens.github.io/Roary/>).

```
Usage: roary [options] *.gff

Options: -p INT    number of threads [1]
        -o STR    clusters output filename [clustered_proteins]
        -f STR    output directory [.]
        -e        create a multiFASTA alignment of core genes using PRANK
        -n        fast core gene alignment with MAFFT, use with -e
        -i        minimum percentage identity for blastp [95]
        -cd FLOAT percentage of isolates a gene must be in to be core [99]
        -qc       generate QC report with Kraken
        -k STR    path to Kraken database for QC, use with -qc
        -a        check dependancies and print versions
        -b STR    blastp executable [blastp]
        -c STR    mcl executable [mcl]
        -d STR    mcxdeblast executable [mcxdeblast]
        -g INT    maximum number of clusters [50000]
        -m STR    makeblastdb executable [makeblastdb]
        -r        create R plots, requires R and ggplot2
        -s        dont split paralogs
        -t INT    translation table [11]
        -ap       allow paralogs in core alignment
        -z        dont delete intermediate files
        -v        verbose output to STDOUT
        -w        print version and exit
        -y        add gene inference information to spreadsheet, doesnt work with -e
        -iv STR   Change the MCL inflation value [1.5]
        -h        this help message

biolinux-ppu@biolinuxppu[Downloads] roary -e --mafft -p 17 AY386263.1.gff3 AY386264.1.gff3 DQ184476.1.gff3 HM133903.1.gff3 KF234407.1.gff3 KP010353.1.gff3 KP010354.1.gff3 KP010355.1.gff3 KP010356.1.gff3 KY053526.1.gff3 LR594616.1.gff3 MG674916.2.gff3 MG712417.1.gff3 MN331655.1.gff3 MN389453.1.gff3 MN454854.1.gff3 KF837136.1.gff3
Use of uninitialized value in require at /usr/lib/x86_64-linux-gnu/perl/5.26/Encode.pm line 61.

Please cite Roary if you use any of the results it produces:
  Andrew J. Page, Carla A. Cummins, Martin Hunt, Vanessa K. Wong, Sandra Reuter, Matthew T. G. Holden, Maria Fookes, Daniel Falush,
  Jacqueline A. Keane, Julian Parkhill,
  "Roary: Rapid large-scale prokaryote pan genome analysis", Bioinformatics, 2015 Nov 15;31(22):3691-3693
  doi: http://doi.org/10.1093/bioinformatics/btv421
  Pubmed: 26198102

2021/01/28 23:58:54 Input file contains duplicate gene IDs, attempting to fix by adding a unique suffix, new GFF in the fixed_input_files directory: /home/biolinux-ppu/Downloads/KF234407.1.gff3
2021/01/28 23:58:54 Input file contains duplicate gene IDs, attempting to fix by adding a unique suffix, new GFF in the fixed_input_files directory: /home/biolinux-ppu/Downloads/KP010354.1.gff3
2021/01/28 23:58:54 Input file contains duplicate gene IDs, attempting to fix by adding a unique suffix, new GFF in the fixed_input_files directory: /home/biolinux-ppu/Downloads/KP010355.1.gff3
2021/01/28 23:58:54 Input file contains duplicate gene IDs, attempting to fix by adding a unique suffix, new GFF in the fixed_input_files directory: /home/biolinux-ppu/Downloads/KP010356.1.gff3
2021/01/28 23:58:54 Input file contains duplicate gene IDs, attempting to fix by adding a unique suffix, new GFF in the fixed_input_files directory: /home/biolinux-ppu/Downloads/KY053526.1.gff3
2021/01/28 23:58:54 Input file contains duplicate gene IDs, attempting to fix by adding a unique suffix, new GFF in the fixed_input_files directory: /home/biolinux-ppu/Downloads/MG674916.2.gff3
2021/01/28 23:58:55 Input file contains duplicate gene IDs, attempting to fix by adding a unique suffix, new GFF in the fixed_input_files directory: /home/biolinux-ppu/Downloads/MG712417.1.gff3
2021/01/28 23:58:55 Input file contains duplicate gene IDs, attempting to fix by adding a unique suffix, new GFF in the fixed_input_files directory: /home/biolinux-ppu/Downloads/MN331655.1.gff3
2021/01/28 23:58:55 Input file contains duplicate gene IDs, attempting to fix by adding a unique suffix, new GFF in the fixed_input_files directory: /home/biolinux-ppu/Downloads/MN389453.1.gff3
2021/01/28 23:58:55 Input file contains duplicate gene IDs, attempting to fix by adding a unique suffix, new GFF in the fixed_input_files directory: /home/biolinux-ppu/Downloads/KF837136.1.gff3
```

**Figure 3.3: Screenshots of the ROARY selected steps. The list of options available to complete an analysis with Roary is shown with the command; the selected steps are surrounded in a red rectangle.**

The GFF3 files were taken as inputs, and coding regions were extracted from the input and converted to protein sequences. Sequences where more than 5% of nucleotides are ambiguous or that are less than 120 nucleotides long were excluded from further analysis. Protein sequences that have 100% identity and a matching length of 100% were iteratively pre-clustered with CD-

HIT (Cluster Database at High Identity with Tolerance). CDhit was then repeated with lower thresholds, reducing by 0.5% down to the user defined threshold (defaults to 98%). If a sequence was found in every isolate it was labeled in the program output as a core gene and was excluded in the BLAST analysis. Next, an all against-all comparison was performed with BLASTP on the reduced sequences with a user defined percentage sequence identity (default 95%). Sequences were then clustered with MCL (Markov Cluster Algorithm). After that, the pre-clustering results from CD-HIT were merged with the results of MCL. Finally, multiple output files were generated with ROARY; which include a spreadsheet detailing the presence and absence of each gene in each isolate (Page et al., 2015). From this list, the variable genes for the human derived ORFV isolates were extracted and subjected to further analysis.

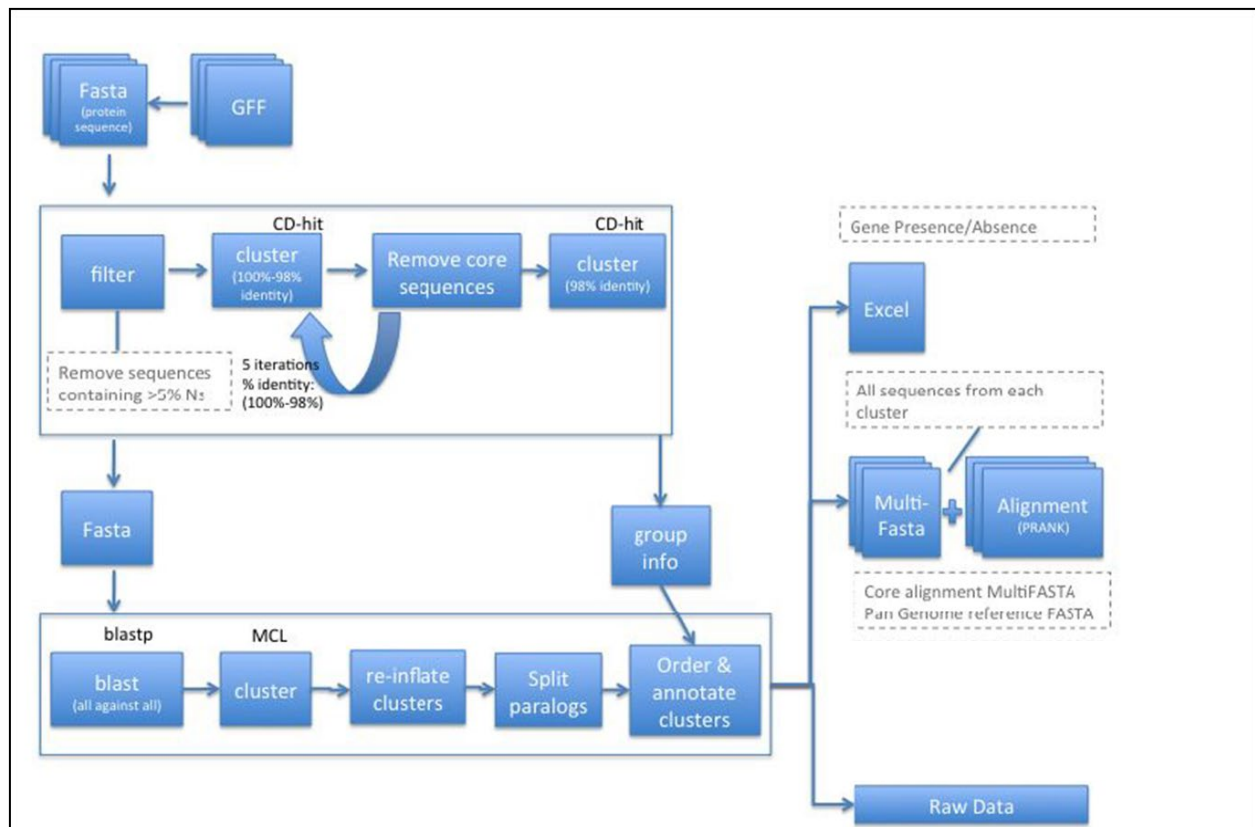


**Figure 3.4: A flowchart of the steps of ROARY application.** Modified from (Page et al., 2015).

### 3.1.4. Multiple sequence alignment and phylogenetic analyses for the selected variable genes

Fifteen variable genes identified using the comparative approach of open reading frames on the complete genomes were analyzed with additional single-gene data to predict molecular

determinants of zoonosis. In this step, genome sequences for each of the fifteen potential candidate genes were retrieved from the GenBank.

Multiple sequence alignments for each candidate gene at the nucleotide and amino acid level were done using MAFFT (Multiple Alignment using Fast Fourier Transform) alignment algorithms in the MEGAX software version .10.18 release #10200331-x86\_64 (S. Kumar et al., 2018). Phylogenetic analyses using MEGAX software were constructed for each selected gene using the Maximum likelihood method with 1000 bootstrap replicates.

### 3.2. Virus isolation and single gene analysis

In addition to ORFV sequences downloaded from the NCBI database, Palestinian sequences were used for some analyses and the collection and processing of these are described (3.2.1 to 3.2.9.), along with the methods of single gene analysis, which was introduced as the final stage of the methodology in the previous section (3.1.4.).

#### 3.2.1. Sample collection and summary of ORFV isolates

Ten ORFV DNA samples were used in this study. They were derived from humans and animals from farms where zoonosis was documented, in the West Bank with contagious ecthyma (**Table 3.2**); two of them were collected previously in 2015 from Jericho and Hebron and stored in a -80°C freezer, while the other four samples were collected in 2019 and 2021 from Bethlehem and Hebron.

**Table 3.2: Palestinian human Orf virus isolates from different regions in West Bank.** Samples 16.1, 16.2 and 18.14 are from two infected brothers. Samples 10.1, 13.1 and 18.38 are from separate cases. Case details are described in section 4.4. N.D. Not documented.

	Sample ID	Sample collection date	Farm location	Host	Age
1	ORF 10.1	Apr,2015	Tubas	Human	Adult
2	ORF 13.1	Sep, 2015	Yatta-Hebron	Human	Adult
3	ORF 14.5	Apr, 2016	Beit Furik-Bethlehem	Goat	Small kid
4	ORF 16.1	Apr, 2016	Beit Furik-Bethlehem	Human	Adult
5	ORF 16.2	Apr, 2016	Beit Furik-Bethlehem	Human	Adult
6	ORF 18.11	May, 2019	Beit Furik-Bethlehem	Sheep	5 months

7	ORF 18.12	May, 2019	Beit Furik-Bethlehem	Sheep	7 months
8	ORF 18.14	May, 2019	Beit Furik-Bethlehem	Human	Adult
9	ORF 18.36	Jan, 2021	Beit Furik-Bethlehem	Lamb	N.D.
10	ORF 18.38	July, 2021	Tafouh, Hebron	Human	Adult

### 3.2.2. ORFV DNA extraction

Scabs that had been collected from infected animals and humans that were expected to contain ORFV were stored in a -80° C freezer overnight, and for DNA to be extracted the protocol "DNA purification from tissues" was used with a QIAamp DNA Mini Kit (QIAGEN). Up to 25 mg of infected tissue was used for each sample and ground mechanically with a mortar and pestle until the scab became a powder, and up to 80µl of PBS was added in a 1.5 micro-centrifuge tube with the addition of 100µl ATL buffer. 20µl of proteinase K was added to the mixture, which was vortexed and incubated in a water bath at 56°C for 2 hrs. During incubation the sample was vortexed two to three times per hour to ensure efficient lyses.

Then 200µl of AL buffer was added to the mixture, which was incubated for ten minutes in a water bath at 70°C. After that, 200µl of (96-100%) ethanol was added to mixture, which was then applied to a QIAamp mini spin column and centrifuged at 6000 x g for one minute. The filtrate was discarded and 500µl of washing buffer (AW1) was added to the column and the centrifugation was done at 6000 x g for one minute then the filtrate was discarded again. The column was then washed with 500µl of AW2 washing buffer and the centrifugation was done at full speed (20000 x g) for three minutes. Finally, the QIAamp mini spin column was placed in a clean micro-centrifuge tube and the elution buffer (AE buffer) was added to the column and left to stand for five minutes and then the column was centrifuged at 6000 x g for 1 minute in order to elute the extracted DNA into the micro-centrifuge tube.

### 3.2.3. Primer design

New primers for the ORFV CBP gene were designed using Primer3 (version 4.1.0) - which can be accessed from (<https://github.com/primer3-org>) -based on conserved regions about 80 bp outside the start and the end of the CBP gene in order to be able to sequence the full length of the gene. Seventeen full lengths CBP ORFV sequences including upstream and downstream flanking

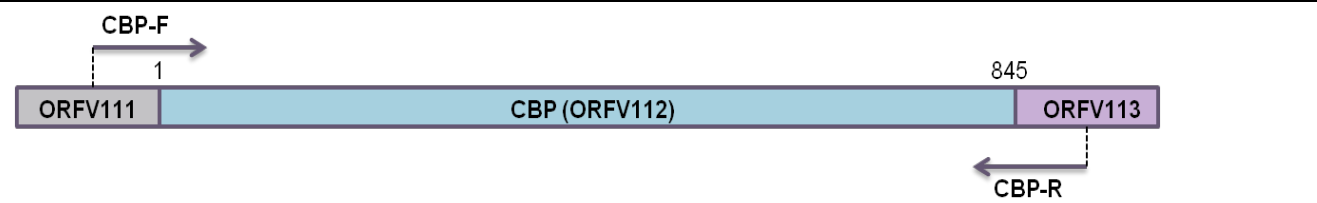


sequences were available from the GenBank database, and these were used to design the primers. They were tested by blast to ensure their specificity for Orf virus.

F1L forward and reverse primers were used for epidemiological study obtained from a previous study (Yang et al., 2014). Their sequences, length, melting temperatures (T<sub>m</sub>) and expected length are described in **Table 3.3**.

Primers were synthesized by Hy laboratories Ltd. Rehovot, and were dissolved in 1x TE buffer to a concentration of 100 pmol/μl, from which working dilutions were made to a final concentration of 10 pmol/μl and these were stored at -20°C until needed.

**Table 3.3: Description of primers for PCR that target the CBP and F1L genes of Orf virus.** The primer sequences, primers lengths, T<sub>m</sub>, and the size of PCR product are shown. Schematic drawing of the CBP primer positions are provided under the set of primers.

Targeted genes	Primer direction	Primer name	Sequence (5'-3')	Length (bp)	Tm (°C)	GC	Size of PCR product (bp)	Reference
CBP	Forward	CBP-F	GCATCCTTGTTTTATCCTGTC	22	58	41.0	1030 bp	This study
	Primer	CBP-R	GCGTTGTGGGATAAGTTTGTG	20	56	45.0		
								
F1L	Forward	F1L-F	ATGGATCCACCCGAAATCACG	21	64	52.4	1023bp	(Yang et al., 2014)
	Reverse	F1L-R	TCACACGATGGCCGTGACCA	20	63	50.0		

### 3.2.4. Polymerase Chain Reaction (PCR) reaction conditions

#### 3.2.4.1. PCR reaction conditions for the CBP gene

Polymerase chain reactions were carried out in a total volume of 25.0μl reaction mixture, which contained 2.5 μl of 10x reaction buffer- Mg<sup>2+</sup> free - Cat. #:37A - Hy-labs, 2.5 μl of 20 mM MgSO<sub>4</sub>- Cat. #:37B - Hy-labs, 0.5 μl of 10 μM dNTPs- Cat. #:RO192 - Fermentas Life Science, 1 μl of 10 pmol/μl of each of the forward and reverse primer working stocks, 1 μl of template DNA, and 0.15μl of Taq DNA polymerase-High Pure (5u/ μl); Cat. #:HTD0078-Hy-labs, 16.35 μl Ultra Pure Water - PCR Grade 100 ml - Fisher biotec /Australia. PCR was performed in a



T100™ Thermal Cycler from Bio-Rad under the following program: Initial denaturation at 95°C for five minutes followed by 35 cycles of 95°C for thirty seconds, 53°C for 45 seconds, 72°C for 45 seconds, and a final extension of 72°C for 10 minutes.

#### **3.2.4.2. PCR reaction conditions for the F1L gene**

The master mix for PCR was carried out in a total volume of 25.0µl, which contained 2.5 µl of 10x reaction buffer- Mg<sup>2+</sup> free, 2.5 µl of 20 mM MgSO<sub>4</sub>, 0.6 µl of 10 mM dNTPs, 1.0µl of template DNA, 0.5 µl of 10 pmol/µl of each of the forward and reverse primer, 0.15µl of Taq DNA polymerase and 17.25 µl Ultra-Pure Water. PCR reactions were performed in a thermocycler T100™ Thermal Cycler from Bio-Rad and the program was set as the following: initial denaturation at 95°C for 4 minutes followed by 35 cycles of 94°C for 50 seconds, 62°C for 45 seconds, 72°C for 90 seconds, and a final extension of 72°C for 10 minutes.

#### **3.2.5. Electrophoresis**

PCR products were analyzed using 1% (W/V) agarose gel electrophoresis -Cat.#: PC0701-500G – Vivantis in 1X TBE buffer -Cat.#:A0024/A0026- Bio Basic, stained with ethidium bromide dye. The voltage power ranged between 100 and 130 volts, and amplicons were visualized as bands under ultra violet (UV) light and photographed using Bio-Rad Molecular Imager® Gel Doc™ XR System. A 100 base pair DNA ladder -Cat.#: DM001-R500- GeneDireX, was used as a DNA molecular weight marker.

#### **3.2.6. Purification and sequencing of PCR products**

The PCR purification kit NucleoSpin® Gel and PCR Clean-up (MACHERY-NAGEL) REF 740609.50 was used for PCR products extraction of amplicons from agarose gels depended on amplicon quality and is described as follows.

PCR products which gave distinct bands without nonspecific products when it was tested in the agarose gel were purified as follows. The PCR reaction was mixed with its double volume of NTI buffer, then a NucleoSpin® Gel and PCR Clean-up column was placed into a 2 ml collection tube and 700 µl of the sample was loaded into it. Centrifugation was done at 11,000 x g for 30 seconds, and then the flow through was discarded and 700µl of washing buffer NT3 was added and centrifuged at the same speed for 30 seconds and again the flow through was discarded. The same washing step was repeated, and then the NucleoSpin® Gel and PCR Clean-

up column was centrifuged at the same speed for one minute. Finally, the NucleoSpin® Gel and PCR Clean-up column was transferred to a new collection tube and then 20µl of NE elution buffer was added onto the center of the column and allowed to stand for one minute. Then the centrifugation was done at 11000 x g for one minute to have the ready to use purified DNA for sequencing. When there were nonspecific bands in the agarose gel in addition to the required band, the PCR products were purified according to the manufacturer's instructions, where a slice of agarose gel (100 mg) containing the required amplification product was cut out of the gel and put into a 1.5 micro-centrifuge tube with 200µl of NTI buffer, followed by incubation at 50°C for 5-10 minutes to dissolve the gel completely. Then the same steps described above were repeated.

### **3.2.7. DNA sequencing:**

The purified DNA products were subjected to sequencing using forward and reverse primers targeting the CBP and F1L genes. The master mix for sequencing was prepared to a total volume of 10 µl reaction mixture, which contained 1.05µl of BigDye Terminator v1.1/v3.1 5x Sequencing Buffer Cat.#:4336697, 2.1 µl of BigDye Terminator v1.1 Ready Reaction Mix Cycle Sequencing RR-100 Cat.#:4336768, 0.5µl of each of forward and reverse primer working stock, 1.5µl of purified DNA and 5.35 µl Ultra Pure Water- PCR Grade 100 ml - Fisher biotec /Australia.

Cycle sequencing reactions were loaded in to a T100™ Thermal Cycler from Bio-Rad under the following program: initial denaturation at 96°C for 1 minute; followed by twenty-five cycles of 96°C for thirty seconds, 53°C for forty five seconds and a final extension 60°C for four minutes. After cycle sequencing was complete, the sequencing reactions were centrifuged for 1 minute and then purified by Applied Biosystem *BigDye® XTerminator™* Purification Kit Cat.#: 4376486; this procedure was carried out according to the manufacturer's instructions.

Into each well of a strip tube, 10 µl of SAM™ Solution and 45 µl of XTerminator™ Solution was added, the strip tubes were sealed using a rubber septa Cat. #: 4306311. Then the contents were mixed for 30 minutes, centrifuged for 2 minutes at 1200 rpm and placed in the Applied Biosystem SeqStudio™ Genetic Analyzer, Medium Seq\_BDX run module was selected from the Software Applied Biosystems run modules for use with the BigDye XTerminator Purification Kit and Data Collection Software.

Sequencher software version 4.5.6 was used for the analysis, manipulation and treatment of sequences and matching of forward and reverse sequences of each sample into a single contiguous sequence.

### 3.2.8. Multiple sequence alignment and phylogenetic analysis

The multiple sequence alignments of nucleotide and amino acid sequences of the full length of CBP and F1L genes were done on Palestinian isolates. They were compared with the ORFV sequences from GenBank using MAFFT (Multiple Alignment using Fast Fourier Transform) alignment tool- available on MEGAX software. Phylogenetic analyses using MEGAX software were constructed using the maximum-likelihood method with 1000 bootstrap replicates.

A total of 40 full lengths CBP ORFV sequences from GenBank database (**Table 3.4**) and 6 full lengths from Palestinian sequences (ORF 10.1, 16.1, 16.2, 13.1, 18.14 and 18.38) were used in this study at the amino acid (**Table 3.2**). Nine of these sequences were taken from infected sheep, eight sequences from humans who caught the infection from infected animals and the remaining sequences (26 sequences) were taken from infected goats. Two sequences are tissue culture adapted, the first isolate is NZ7 (AAR18811.1) which was twice plaque purified in bovine testis cells and then reinoculated into sheep (Robinson et al., 1987), the second isolate is vaccine isolate strain TVL (QJX15539.1) which derived from cell culture infected with contagious ecthyma vaccine (Heare et al., 2020). These isolates were collected between 1996 and 2021 from different regions in the world.

A total of 17 full lengths F1L sequences came from the ORFV complete genome in the GenBank database (**Table 3.1**) and 7 full lengths from Palestinian isolates ORF 16.1, 16.2, 14.5, 18.11, 18.12, 18.14 and 18.37 (**Table 3.2**) at nucleic acid levels were used in this study.

**Table 3.4: GenBank accession number of Orf virus isolates which have the full length of CBP gene with host, country and year of collection. (a.a amino acid).**

	Accession number (a.a)	Host	Country	Year
1	AA091821.1	Sheep	Netherlands	2003
2	AHJ61508.1	Goat	China	2010

3	AWA82556.1	Goat	China	2017
4	AWA82557.1	Goat	China	2016
5	AWA82558.1	Goat	China	2015
6	AWD31696.1	Goat	China	2013
7	ASL69136.1	Goat	China	2014
8	ASL69137.1	Goat	China	2014
9	ASL69138.1	Goat	China	2015
10	ASL69139.1	Goat	China	2016
11	ASL69140.1	Goat	China	2016
12	ASL69141.1	Goat	China	2017
13	AWN09358.1	Goat	India	2005
14	AWN09359.1	Goat	India	2005
15	AWN09360.1	Goat	India	2004
16	AWN09361.1	Goat	India	2003
17	AWN09362.1	Goat	India	2014
18	AWN09363.1	Goat	India	2008
19	AWN09364.1	Goat	India	2006
20	AWN09365.1	Sheep	India	2006
21	AWN09366.1	Goat	India	2006
22	AWN09367.1	Goat	India	2005
23	AHH34297.1	Human	Germany	1996
24	AKU76734.1	Sheep	Germany	2010
25	AKU76990.1	Goat	China	2012
26	AKU76602.1	Goat	China	2012
27	AKU76866.1	Goat	China	2012
28	AHZ33810.1	Goat	China	2012
29	QLI57620.1	Sheep	China	2018
30	QLI57751.1	Sheep	China	2017
31	AYM26053.1	Sheep	China	2016
32	AYN61060.1	Goat	China	2016

33	ASY92409.1	Sheep	China	2012
34	ABA00630.1	Sheep	China	2005
35	AAR98207.1	Sheep	New Zealand	2005
36	AAR98337.1	Sheep	USA	2003
37	QJX15532.1	Tissue culture	USA	2019
38	VTU03255.1	Human	France	2017
39	QQY02738.1	Goat	India	2017
40	AAR18811.1	Tissue Culture	New Zealand	2004

### 3.2.9. Sequence logo generation

Graphical representations of amino acid sequence variation were generated using the WebLogo server (<https://weblogo.berkeley.edu/logo.cgi>). The amino acids sequence for human ORFV CBP and for small ruminants ORFV were entered in a certain box in this web page then the sequence logo will show how well residues are conserved at each position and different residues at the same position are scaled according to their frequency (Crooks et al., 2004).

## CHAPTER (4)

### 4. Results

From the GenBank database, 17 complete ORFV genomes that had been isolated from human and animal hosts were used to search for molecular markers of zoonosis in the ORFV genome. Using first a comparative genomic approach, 15 candidate genes were identified, and these were narrowed down further through a pipeline of discrimination to 1 gene (CBP) could play a role in ORFV zoonosis. Results are summarized in **Figure 4.1**.

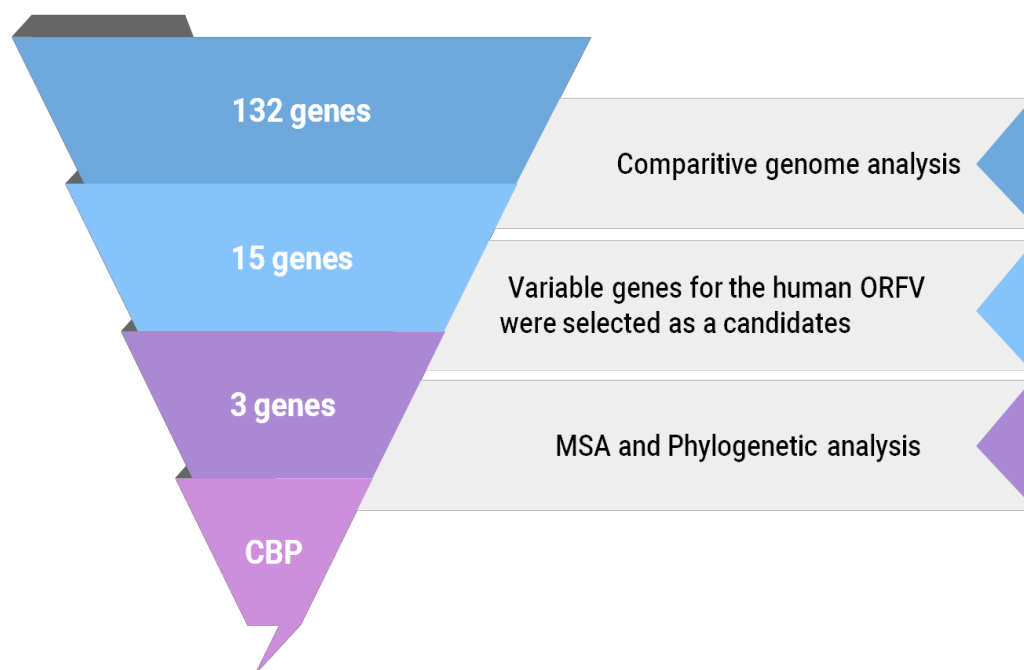


**Figure 4.1:** Summary of the resulted genes in each step of the pipeline for molecular marker candidates' criteria.

## 4.1 Comparative genome analysis

Using ROARY with its default parameters using 95% similarity for BLASTP, 15 genes were found to be potential candidate markers for human derived ORFV isolates in **table 4.1** (KF837136.1 and LR594616.1). The comparison was applied to similar genomes, in order to find a distinction between isolates that could be associated with host preference.

**Table 4.1: Potential candidate genes list.**

#	Open reading frame	Protein product	Symbol
1	ORF001	Hypothetical protein	
2	ORF005	Hypothetical protein	
3	ORF007	Deoxyuridine 5-triphosphate	dUTPase
4	ORF012	Hypothetical protein	
5	ORF017	DNA-binding phosphoprotein	
6	ORF046	Putative myristylated protein	L1R
7	ORF056	RNA polymerase subunit	
8	ORF059	Immunodominant protein	F1L
9	ORF080	Hypothetical protein	
10	ORF088	Hypothetical protein	
11	ORF109	Extracellular envelope glycoprotein	EEV
12	ORF112	Chemokine-binding protein	CBP
13	ORF116	Hypothetical protein	
14	ORF120	Hypothetical protein	
15	ORF132	Vascular endothelial growth factor-like protein	VEGF

## 4.2. Multiple sequence alignment and phylogenetic tree of candidate genes

Comparative sequence analysis of the 15 potential species-specific genes that were detected from the previous step (**Table 4.1**) was carried out using MEGAX. The phylogenetic tree based on the dUTPase, EEV glycoprotein and CBP nucleotide sequences showed human derived isolates falling within one cluster with a high bootstrap value: 66, 95 and 99%, respectively (**Figures 4.2,**

4.3 and 4.4). However, multiple sequence alignment and phylogenetic trees that are based on the other potential candidate genes failed to display any branches for human derived ORFV that were distinct from small ruminants (See **figures S1-S12**). There were no non-conservative substitutions in the dUTPase, while EEV had 7 and CBP had 12 amino acid substitutions that distinguished the 2 human-derived genomes from the rest, and the CBP gene was selected for single gene analysis.

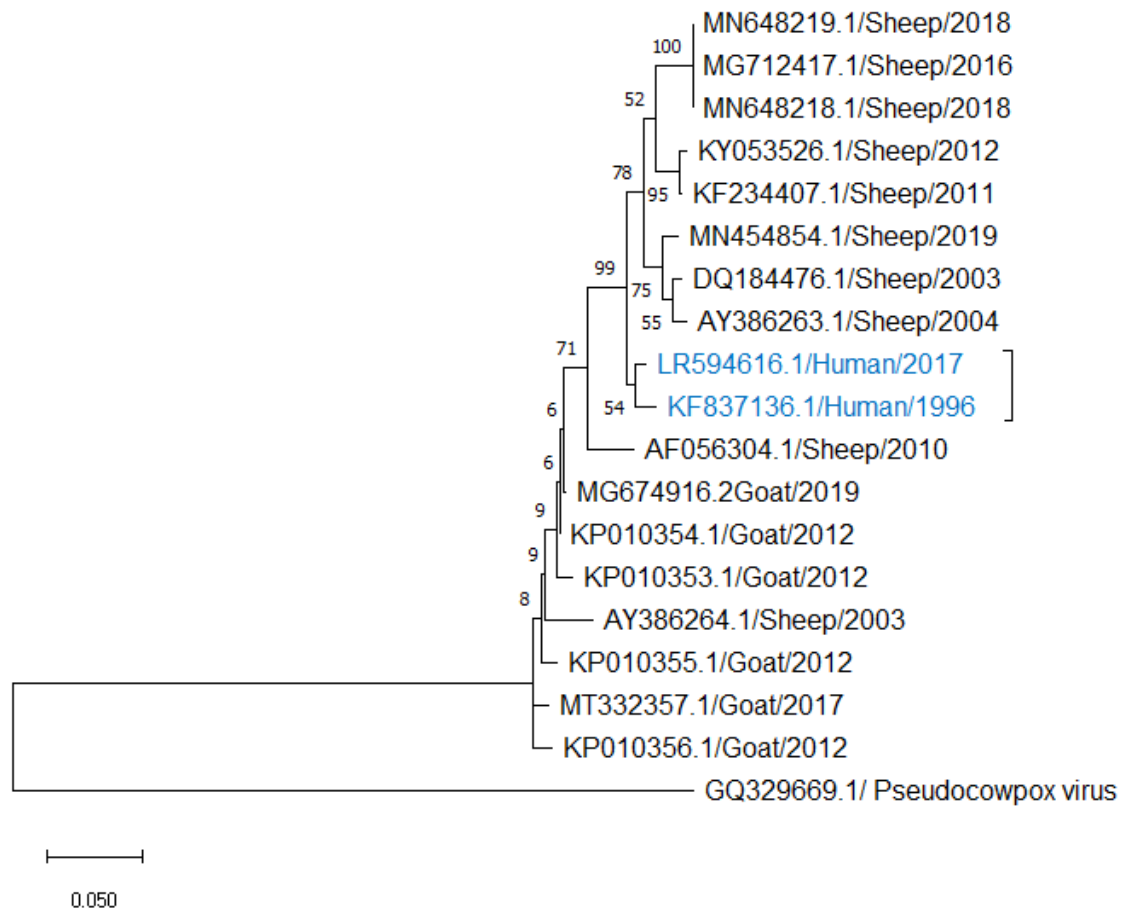


**Figure 4.2: Phylogenetic analysis based on dUTPase nucleotide sequences.** Maximum likelihood method was used for analysis with a bootstrap test (1000 replicate). The tree was built from 35 sequences retrieved from GenBank. In addition, the homologue gene sequence of GQ329670.1 (Pseudocowpox virus) was used as an out-group. The tree is drawn to scale, with branch lengths in the same units as those of the evolutionary distances used to infer the phylogenetic tree. The human derived ORFV isolates are highlighted in blue.



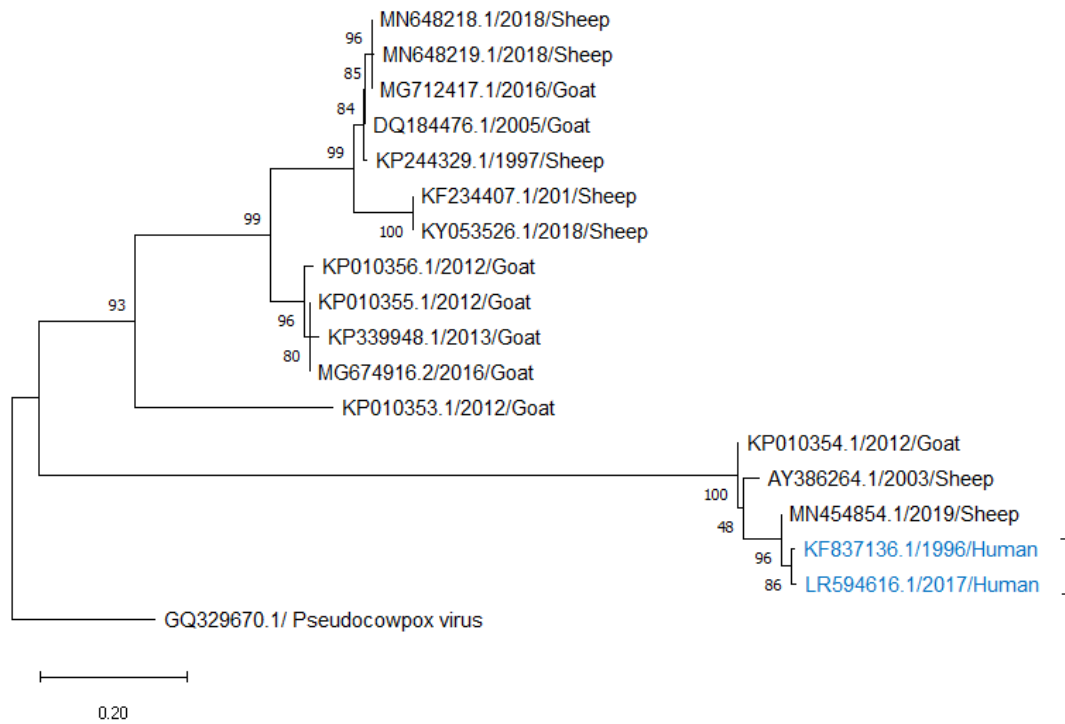


**Figure 4.3: Phylogenetic analysis based on EEV glycoprotein nucleotide sequences.** Maximum likelihood method was used for analysis with a bootstrap test (1000 replicate). The tree was built from 22 sequences retrieved from GenBank. In addition, the homologue gene sequence of GQ329670.1 (Pseudocowpox virus) was used as an out-group. The tree is drawn to scale, with branch lengths in the same units as those of the evolutionary distances used to infer the phylogenetic tree. The human derived ORFV isolates are highlighted in blue.

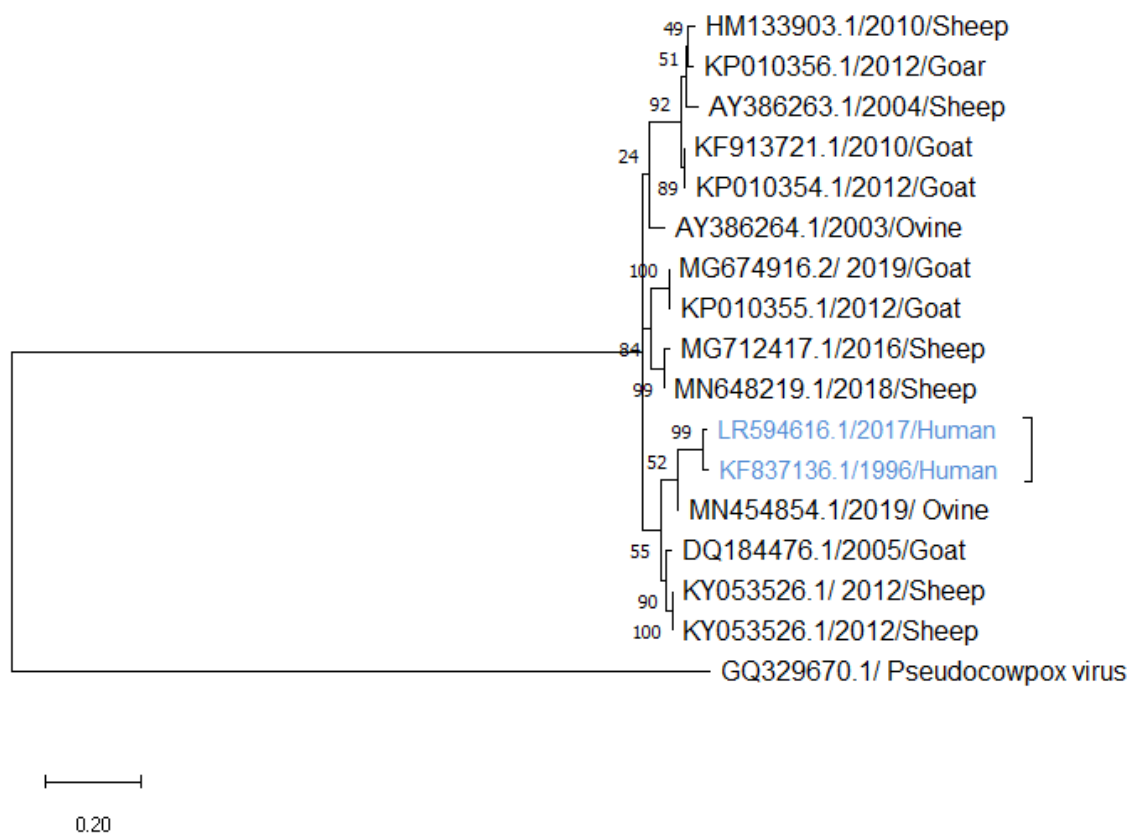


**Figure 4.4: Phylogenetic analysis based on CBP nucleotide sequences (867nt).** Maximum likelihood method was used for analysis with a bootstrap test (1000 replicate). The tree was built from 18 sequences retrieved from GenBank. In addition, the homologue gene sequence of GQ329670.1 (Pseudocowpox virus) was used as an out-group. The tree is drawn to scale, with branch lengths in the same units as those of the evolutionary distances used to infer the phylogenetic tree. The human derived ORFV isolates are highlighted in blue.

### 4.3. CBP gene based analysis

#### 4.3.1. Amplification of the CBP gene from local human ORFV isolates

To test the hypothesis that the CBP gene from ORFV that infects humans is distinct from that infecting small ruminants more sequence data, especially from human isolates, was sought. Successful amplification of the CBP gene from previously verified ORFV DNA of Palestinian isolates was achieved with primers designed to amplify, for the first time, the full length CBP

gene as shown in **Figure 4.5**. The band size for the amplicon was approximately 1030 bp, which covers the full length of the 887bp CBP gene along with 5' and 3' flanking sequences. The CBP gene in the six Palestinian human-derived ORFV samples was sequenced after its amplification (**Table 3.2**).

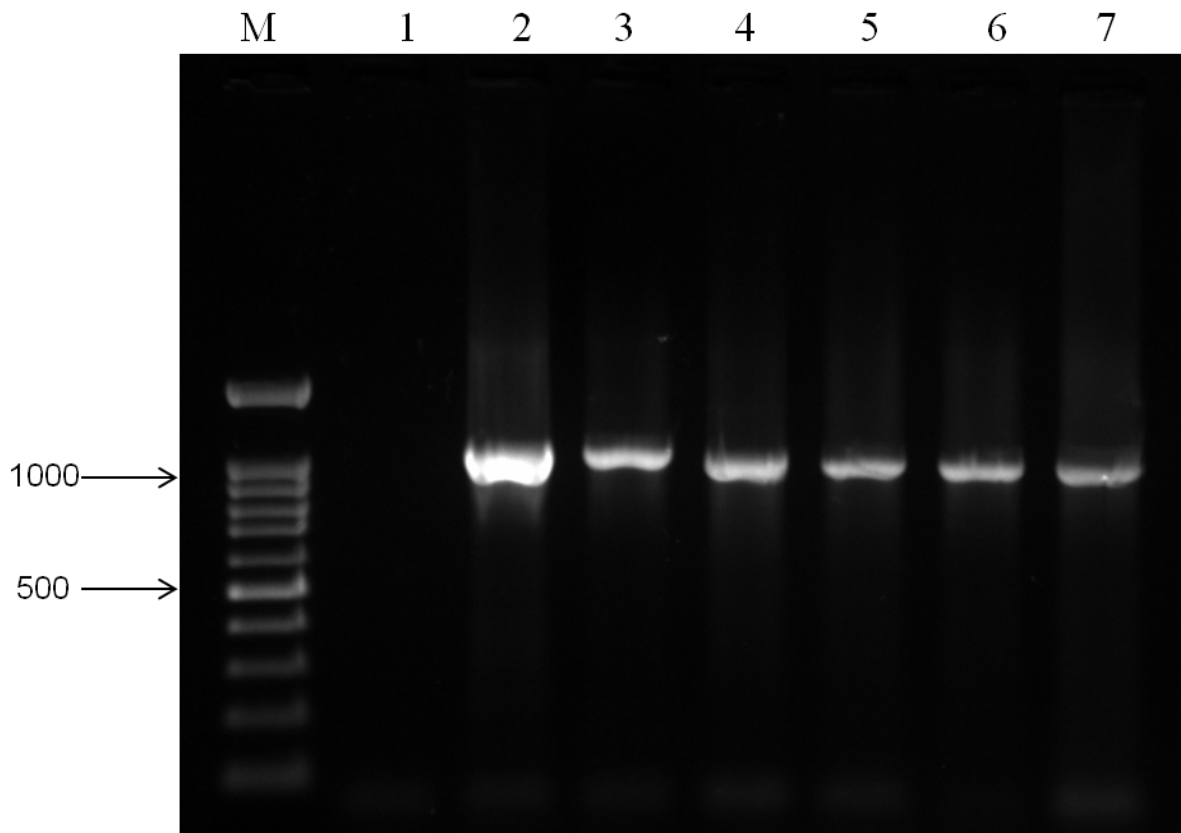


**Figure 4.5:** A representative Agarose gel electrophoresis of 1030bp of the full length CBP gene of ORFV amplified by PCR on 1% Agarose. Lane M: 100 bp DNA ladder (GeneDireX), lane 1: No Template Control (NTC), lane 2: ORF 18.11 as a positive control and lanes 3: ORF 18.14, lane 4: ORF 16.1, lane 5: ORF 16.2, lane 6: ORF 10.1 and lane7: ORF13.1.

#### 4.3.2. Phylogenetic analysis of the full length CBP gene including Palestinian isolates

Comparative sequence analysis of the CBP gene from Palestinian ORFV isolates was carried out including 40 ORFV CBP sequences that were retrieved from GenBank database (**Table 3.4**) using MEGAX. In the phylogenetic tree reconstructions, based on the amino acid sequences of

the CBP gene, the human ORFV isolates are grouped into four major branches. Branch I included three human ORFV isolates, whereas two other local human ORFV isolates separated into two different branches II and III and other three human isolates fell within branch IV, two of them are foreign ORFV strains from Germany and France which are represented by triangles (Figure 4.6).

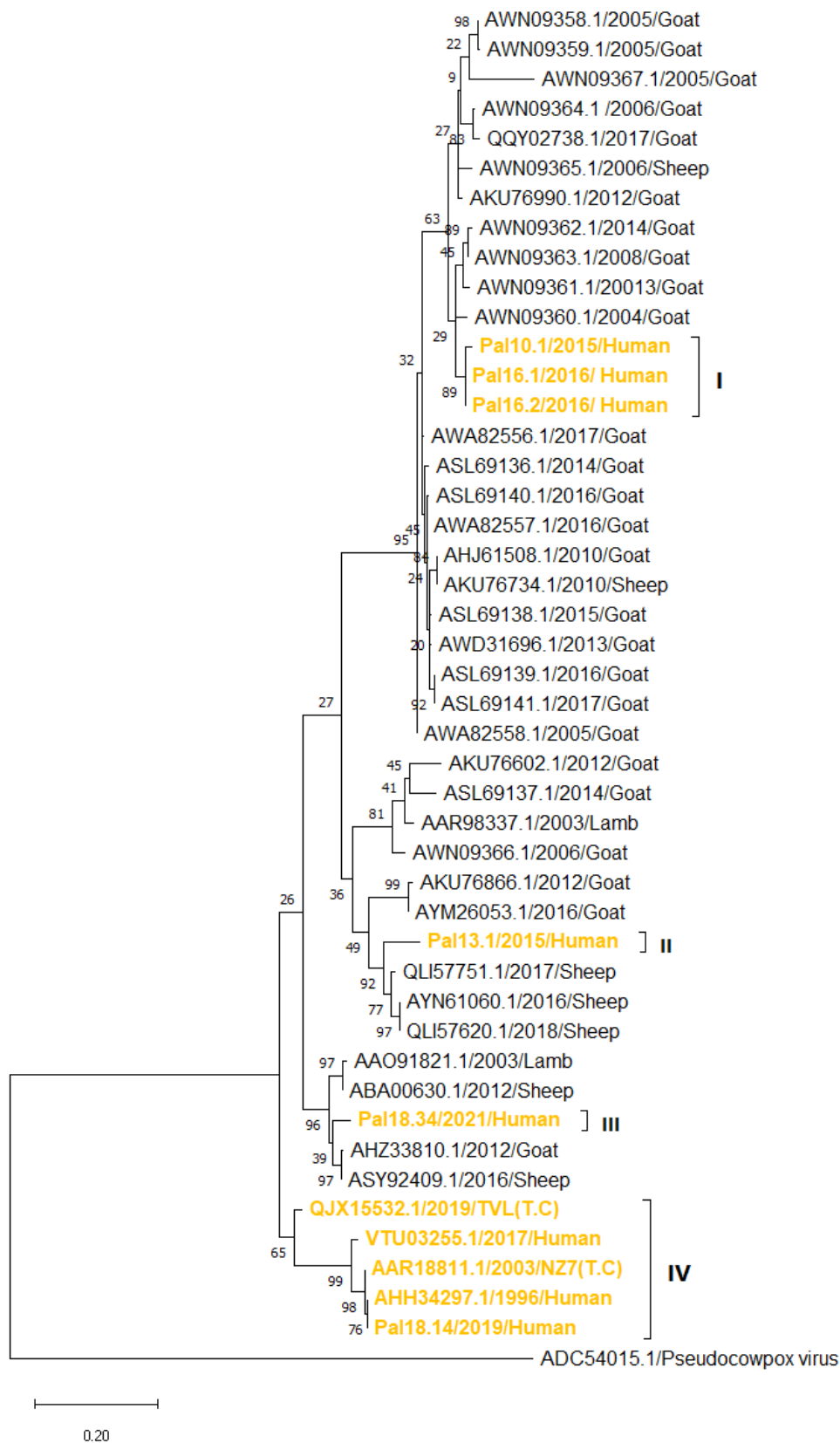


**Figure 4.6: Phylogenetic analysis based on CBP amino acid sequences.** Maximum likelihood method and JTT matrix-based model was used for analysis with bootstrap test (1000 replicate). The tree was built from 46 derived amino acid sequences including 6 Palestinian sequences with outgroup (ADC54015.1) for rooting the tree. The tree is drawn to scale, with branch lengths in the same units as those of the evolutionary distances used to infer the phylogenetic tree. The human ORFV isolates were highlighted in the four different branches.

### 4.3.3. Species specific amino acid variations in the CBP protein

Twelve amino acid substitutions were identified as species specific markers that distinguish human from small ruminant derived ORFV by multiple sequence alignment of 46 isolates of ORF112 CBP protein isolates, which includes Palestinian isolates (**Figure 4.7**).

In the alignment (**Figure 4.7A**), a complete block of 12 novel amino acid substitutions was unique to three (18.14, VTU03255.1, AHH34297.1) of 7 human ORFV isolates compared to the small ruminant consensus sequence. Of the remaining 4 human ORFVs, three shared identity to the consensus sequence for small ruminants at these positions, while one (18.38 isolate) shared 2 of the 12 substitutions: Q38H and G160D, while at the other 10 sites the sequence was the same as the consensus for small ruminants.

Out of human samples, other substitutions found were at amino acid positions V60T, V73M and E/T135A in human isolates 13.1 and 18.38. In addition, all the 12 substitutions were also detected in two isolates derived from tissue culture: the AAR18811.1 isolate and 5 out of 12 (M73T, K135A, V150D, G160D and R229G) were found in the QJX15532.1 isolate.

The consensus sequences of all twelve positions of the CBP multiple sequence alignments across 37 small ruminant isolates were depicted as a sequence logo where each site is represented as a stack comprising each of the amino acid residue polymorphisms and the height of each stack indicates the degree of conservation (**Figure 4.7B**). The height of each letter within a stack represents the relative frequency of that amino acid residue. It can be seen the positions K30, E40, R46, P57, V150 and R229 are highly conserved, while other remaining positions 28, 38, 60 and 160 are comparatively conserved.

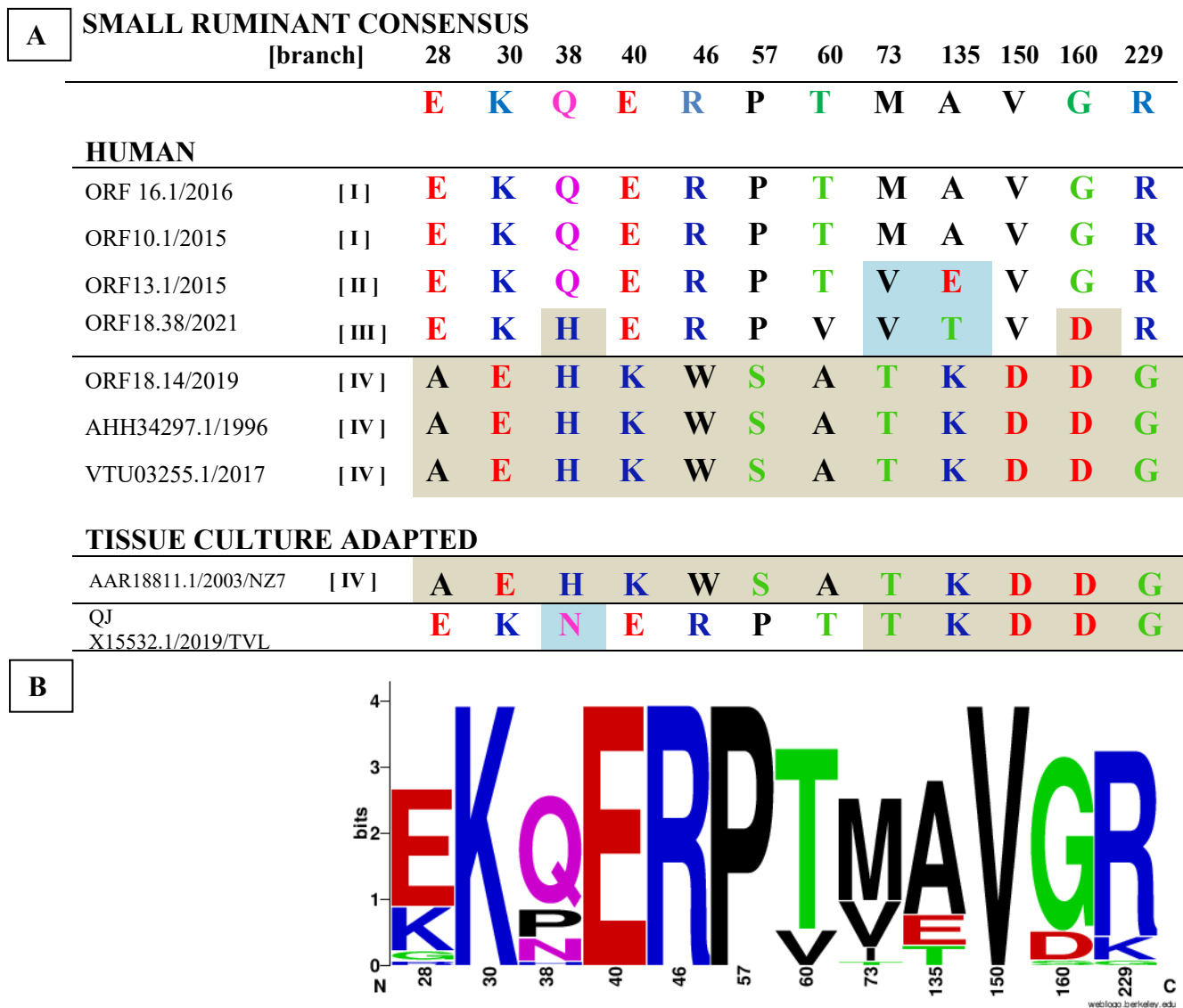


**Figure 4.7: Species specific markers for CBP at the amino acid level for 12 sites.** A) Schematic representation of an MSA for 7 human and 2 tissue culture adapted (NZ7 and TVL) ORFV isolates compared to a small ruminant consensus. Substitutions common to branch 4 of the tree (Figure 4.6) are shaded grey, and other substitutions are shaded in pale blue B) Sequence Logos of the CBP multiple sequence alignments across 37 small ruminants isolates.

## 4.4. Case presentation

### 4.4.1. Recurrent zoonotic infection from the same Palestinian farm

ORFV infection emerged for the first time in 2016 on a new farm in Bethlehem-Palestine after importing goat-kids from Israel. Transmission to two brothers working on the farm occurred at that time and again subsequently from a flock of sheep to one of the brothers in 2019 as shown in **Figure .48.**

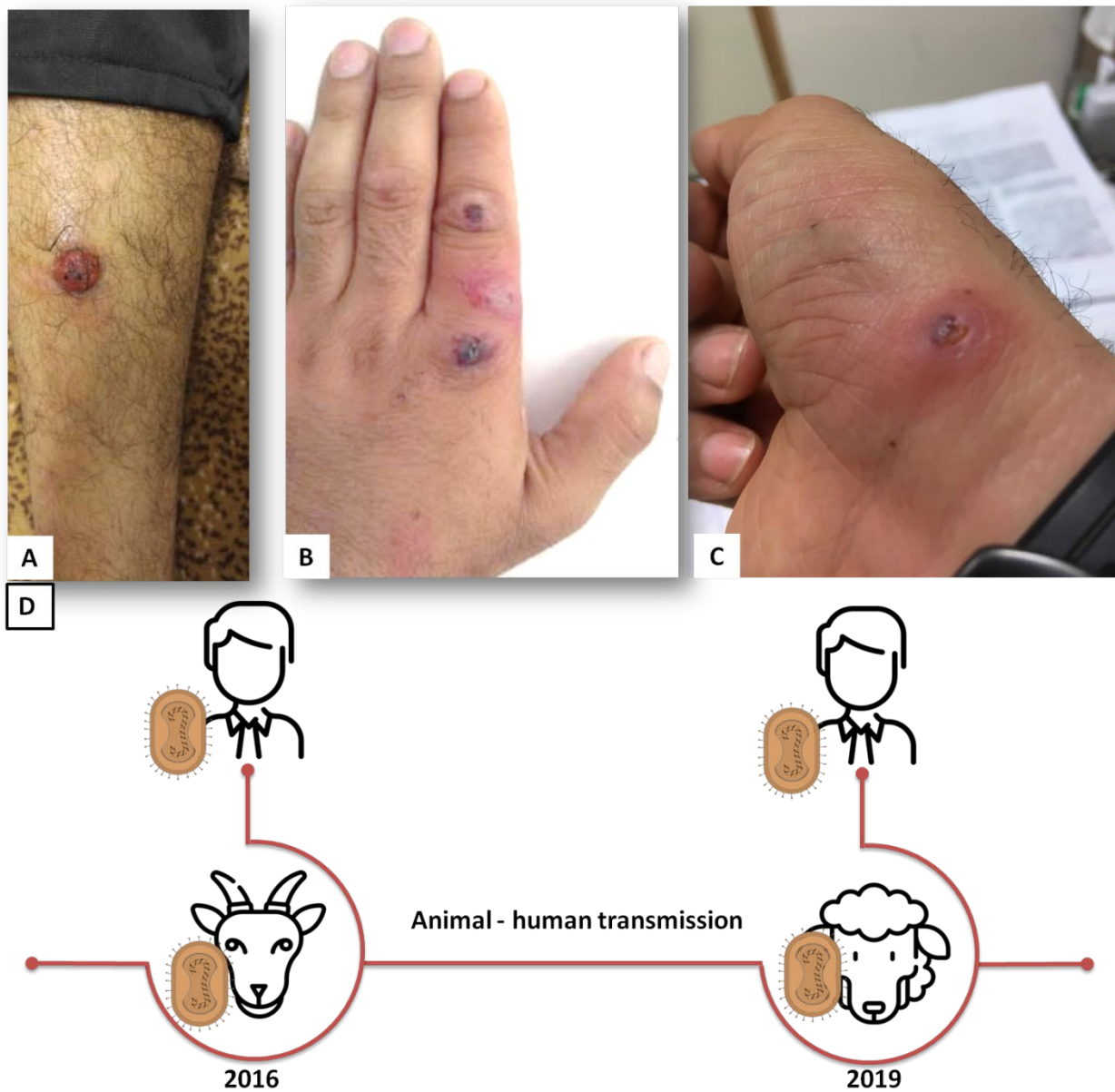




**Figure 4.8: Clinical presentations of Orf lesions in the 2 brothers.** A) Large red papule on the leg of case-patient 2, B) lesions on the index finger of the veterinarian of case-patient 1, C) erythematous lesion on the hand of case-patient 1, D) Schematic overview of the history of zoonotic ORFV transmission.

### **Outbreak 1 (2016):**

In April 2016, two brothers had painful lesions simultaneously after contact with goat kids on their farm, where the goats and humans were diagnosed as being infected with ORFV.

**Case 1**, (ORF16.1), a 30-year-old male brother of case-patient 1, a farmer, presented with a large red papule of 15 mm on his right leg that first appeared after he incurred an injury while working in the farm. The lesion was first observed approximately two weeks previously (**Figure .48A**). He had a slight fever, and itching all over his leg before noticing the growth formation for about one week, followed by malaise for about three days and which became increasingly firm and painful. The lesions were evaluated by a physician, and described as undetectable infection. No supplementary investigations were performed and the treatment performed focused on pain management, through the use of general analgesic and a course of antibiotics. The lesion began to dry and shrink after three days and had healed completely after six weeks.

**Case 2**, (ORF16.2), a 32-year-old male, a veterinarian, presented with two small, initially well-defined lesions of 13 and 7 mm in diameter on his index finger in his left, appeared after seven days of his injury when he was working with utensils and wires in the farm (**Figure .48B**). Three days later, the lesions were described as itchy, erythematous, and swollen. After four days, a painful and itchy erythematous oval thickening area about 16 mm long and 11 mm wide has formed. The patient visited the same previous physician who diagnosed the case as undetected infection and prescribed analgesic drugs. Regression of the lesions was complete by eight weeks, leaving small scars at the sites of infection.

### **Outbreak 2 (2019):**

**Case 3**, (ORF18.14), in May 2019, one of the brothers got reinfected with ORFV after contact with infected sheep. The patient presented with a lesion without local complications on his right hand. The lesion was erythematous and swollen (**Figure .48C**).

**In January 2021**, a third outbreak occurred in the farm, but without zoonotic transmission.

#### **.44.2. Other zoonotic cases**

**Case 4, (ORF 10.1/2015)**, a veterinarian in Jenin, Palestine, presented with mouth sore. The infection occurred approximately three days after intensive handling of ORFV lesions for autologous vaccine preparation. The complete regression of the lesions took 22 days.

**Case 5, (ORF 13.1/2015)**, skin scab obtained from a patient who visited a dermatologist for diagnosis in Hebron, Palestine, and no additional information available.

**Case 6, (ORF 18.38/2021)**, a 30-year-old male in Taffouh-Hebron, Palestine presented with a skin lesion on his hand. Approximately two weeks before the presentation, he had punctured his right hand with a knife while skinning a sheep. He recalled that it had pimple-like lesions on its lips. One week later, he developed skin lesions on his middle finger in his right hand overlying the dorsal surface of the joint. The lesion initially started as localized erythema and progressed to become painful and swollen, restricting joint movement (**Figure 4.9**). He had fevers, chills and itching with secondary bacterial infection. The lesion was evaluated by several physicians described as an infection of unknown type, and only one physician was able to diagnose it as ORFV infection. The treatment performed focused on pain management and a course of antibiotics. After 15 days, the lesion had significantly improved, with resolution of swelling and pain.



**Figure 4.9: Clinical presentations of orf lesion stages in case 6.** **A)** acute weeping nodule on the dorsal third digit of the right hand overlying the proximal interphalangeal joint, **B)** Targetoid plaque with central necrosis, **C)** Violaceous, dome-shaped nodule with central dusky blue hue and fissure as well as peripheral rim of erythema, **D)** The lesion was healing in the regression stage, which is characterized by dry crust.

## 4.5. F1L gene based analysis

### .45.1. Amplification of the F1L gene from ORFV isolates in the three outbreaks

The F1L gene was amplified from the three outbreaks in the farm including human isolates from case 1, 2 and 3 (16.1, 16.2 and 18.14) and animal isolates (ORF 14.5, 18.11, 18.12 and 18.36) in **Table 3.2**. The seven Palestinian ORFV samples were confirmed as ORFV infections in humans and kids and were sequenced after its amplification. Representative results (**Figures 4.10**) of PCR products from outbreak 1 and 2 are shown below.

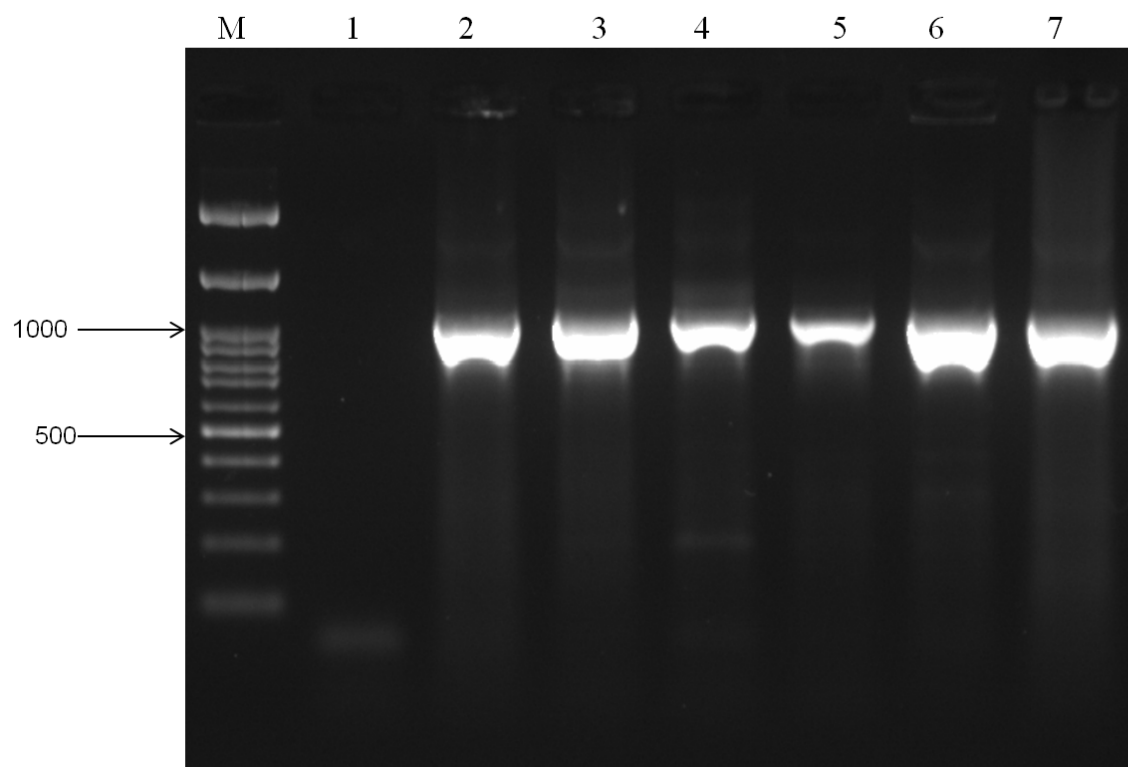


**Figure 4.10: A representative Agarose gel electrophoresis of 1005bp of the full length F1L gene of ORFV amplified by PCR on 1% Agarose. Lane M: 100 bp DNA ladder (GeneDireX), lane 1: No Template Control (NTC), lane 2: ORF 18.11 as a positive control, lanes 3: ORF18.12, lane 4: ORF18.14, lane 5: ORF16.1, lane 6: ORF16.2 and lane7: ORF14.5.**

#### **.45.2.Phylogenetic analysis of ORFV based on the full length F1L gene**

Comparative sequence analysis of the Palestinian ORFV isolates (where 3 isolates came from human, 3 from sheep, 1 from goat and 1 from lamb) based on the full length of the F1L gene was carried out including 18 F1L sequences of the ORFV complete genomes from the GeneBank at the nucleic acid level (**Table 3.1**) using MEGAX.

Multiple sequence analysis indicated 95.4-96.8% and 94.7-96.7% sequence identities among Palestinian ORFV isolates at the nucleotide and amino acid level, respectively. A notable 24 nucleotides deletion/insertion at nucleotide position 130-135 and 163-180 (the numbers refers to the alignment) was observed in the 5' end coding for proline rich repeating motif (**Figure S.13**).

Phylogenetic analysis based on the F1L gene sequences categorizes the three ORFV recurrent infection sequences into two distinct branches, where branch I including the outbreak 1 and 3 infection strains of goat origin, and branch II including the outbreak 2 infection of sheep origin (Figure 4.9).

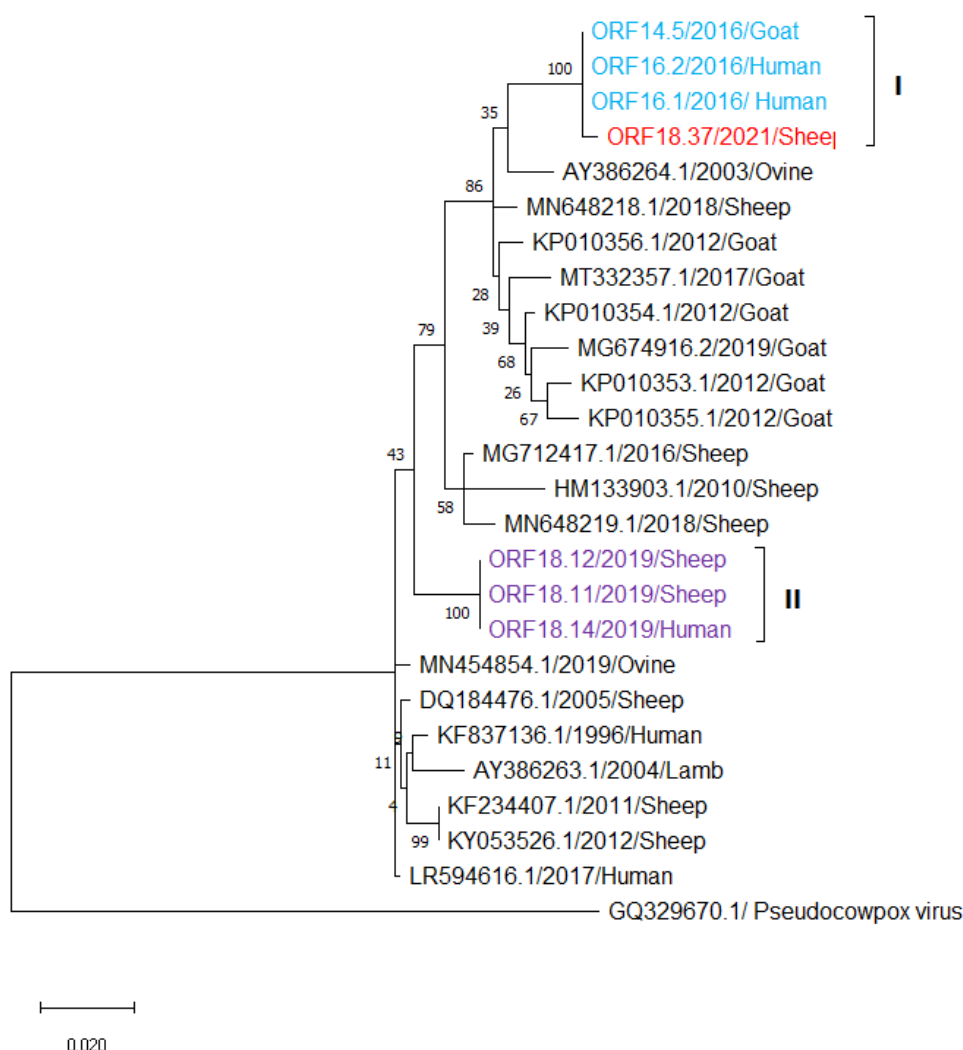


**Figure 4.11: Phylogenetic analysis based on F1L nucleotide sequences distinguishing the viral strain in the three infections.** Maximum likelihood method was used for analysis with a bootstrap test (1000 replicate). The tree was built from 25 derived nucleotide sequences including 7 Palestinian sequences with outgroup for rooting the tree. The tree is drawn to scale, with branch lengths in the same units as those of the evolutionary distances used to infer the phylogenetic tree. The first outbreak highlighted in blue, second outbreak highlighted in purple, and red highlight for the third outbreak.

## CHAPTER (5)

### 5. DISCUSSION

ORFV is a zoonotic disease, transmitted to humans from small ruminants through the skin, and while it is not fatal, it causes painful lesions. Humans are predominantly dead-end hosts, but numerous zoonotic infections with ORFV have been reported worldwide, mainly in developing countries (Kassa, 2021). Understanding determinants of successful cross-species transmission could help in the early prediction and prevention of future pandemic zoonoses. Several studies have identified species specific marker genes that cluster the ORFV strains depending on whether the host is goat or sheep (Chi et al., 2015; Xiong Wang et al., 2018), and one study reported a species-specific clustering of human-derived ORFV genomes into one clade. This study showed that human ORFV genomes differ by 3.58-4.02% from other animal-derived ORFV genomes (Andreani et al., 2019). However, to our knowledge, the specific viral determinants of ORFV zoonosis have not been investigated at the gene by gene level.

This study was designed to identify molecular determinants in known protein-coding genes of ORFV obtained from zoonotic infections. A combined comparative genome analysis with rational selection steps and phylogenetic analysis was performed to determine potential candidate genes that may play a role in ORFV zoonosis. As a result, among the open reading frames with non-synonymous mutations that are associated with human-derived ORFV isolates, this gene was selected as a potential candidate gene that could play role in ORFV zoonosis

Comparative genomic approach guided the identification overall genomic variation within 17 different ORFV isolates. However, as only two human gene sequences were available from the NCBI database, isolates from local zoonoses were collected for DNA isolation and sequencing during this project to determine if these associations with zoonosis held true for Palestinian zoonotic events, and hence infer how important the identified markers in this gene could be generally.

The full length of this gene sequence when aligned with deposited ORFV sequences downloaded from NCBI database showed similarities with the reference sequences at both nucleotide and amino acid levels. The amino acid identity and similarity of the ORFV proteins are 78% and 87%, respectively. A notable insertion/deletion at amino acid position 78-96 (the

numbers refers to the alignment) was observed (Fleming et al., 2017; Seet et al., 2003). The isolates ORF 18.14 CBP protein is 293 amino acids while Pal 16.1 protein is 281 amino acids. These differences explain differences observed on electrophoretic gel where some isolates were longer than others (**Figure 4.5**).

Remarkably, twelve non-synonymous substitution events were detected as a block in the ORFV amino acid sequences of each of 3 viruses that have been isolated from humans in three different countries, while the other five human isolates show amino acids which were similar to the consensus sequence from small ruminants (**Figure 4.7**). Additionally, the human isolate (ORF18.38) had two of the twelve marker sites in common with the three isolates that had the whole block of 12 unique sites.

Another thing observed was that all of the human host markers were detected also in two isolates: New Zealand, called NZ7 (AAR18811.1) and TVL (QJX15539.1) strain (Heare et al., 2020; Robinson et al., 1987). However, sequence changes in these two isolates may have been selected as a result of selective pressures during the adaption of viruses to either an adherent or a suspension cell culture, and this alterations can lead to influence the cellular tropism and stability of the virus particle (Dill et al., 2018; Portillo et al., 2011). In other words, there is a pattern of sites specific to viruses that have been isolated from non-ruminant sources: whether directly from humans or following adaptation to tissue culture in the laboratory.

The binding sites for across chemokine divided into three regions based on ORFV secondary structure and electrostatic surface potentials. Regions I and II form negatively charged groove, this binding site is formed by a cluster of acidic residues from  $\alpha$  helix 2 and  $\beta$ -sheet II. While region III comprises an extensive hydrophobic surface comprises a highly conserved cluster of hydrophobic residues from  $\beta$ -sheet I and  $\beta$ -sheet II (Couñago et al., 2015). The largely negative and hydrophobic regions of are essential for ligand engagement specifically localized on  $\beta$ -sheet II. There are extensive interactions with the chemokine ligands at this site, which result in a high affinity for most chemokines. Four of the twelve substitutions associated with a clade of human-derived ORFV sequences in this study were mapped into these binding sites in protein that had been previously described (Couñago et al., 2015).

Three substitutions were found in the negatively charged groove: M73T in the  $\beta$ 2 strand and R229G in the  $\beta$ 7-  $\beta$ 8 loop were located in the  $\beta$ -sheet II, and G160D was located in the  $\alpha$ 2 helix. The residues changed from hydrophobic to hydrophilic at positions 73 and 160, while at 229

position the residue changed from hydrophilic to hydrophobic and these changes could affect the structure to some extent, and hence indirectly binding, as the hydrophobic residues tend to be buried in the hydrophobic core, the hydrophilic residues are usually exposed to the surface of the protein.

One substitution found in the  $\beta$ 1 strand, hydrophilic basic arginine (R) changed to hydrophobic tryptophan (W) at highly conserved position 46; this substitution can cause a change in  $\beta$ -sheet I charge. The ORFV has positively charged groove located on  $\beta$ -sheet I which shares distinct homology with the characterized GAG binding site of other viruses such as myxovirus and vaccinia virus in binding to GAGs through positively charged residues. These positive charged residues in  $\beta$ -sheet I is a prominent feature that could interact with GAGs (Couñago et al., 2015; Seet et al., 2003).

Furthermore, five of the substitutions occurred in highly conserved positions. Lysine (K) which is a basic residue and changed to acidic residue glutamic acid (E) at amino acid position 30, while vice versa occurred at position 40. At positions 46 and 150, the residues changed from hydrophilic to hydrophobic, while at 57 position the residue changed from hydrophobic to hydrophilic. Thus, the mutation in these places could produce some changes in structure which could modulate the binding to chemokines.

The primers that were published in previous studies for amplification and sequencing were targeted precisely to the beginning and end of the gene (Fleming et al., 2017; Seet et al., 2003). However, this would have led to the loss of true sequence information in the terminal targets of each PCR primer, which previous studies have not recognized. To correct this oversight in experimental design of previous studies, a new set of primers was designed about 80bp upstream and downstream from the start and the end, respectively, of the gene in conserved regions.

In this study, a novel spate of zoonotic events is reported where two cases of ORFV infection in two brothers who had contact with animals on the same farm occurred in 2016, followed by a new case in one of the brothers during a separate outbreak on the same farm in 2019 (**Figure 4.8D**). The first infection in 2016, the two brothers got the infection from the same source (infected goats) with different clinical manifestations. In the case 1 the lesions appeared in a covered area (leg), indirect transmission through contaminated hands or clothing was the cause of this infection, where in the case 2 it appeared on the hand which was exposed to cuts and



direct contact with the infectious agent. The recurrent infection in 2019, case 3 reinfected with ORFV after direct contact with an infected sheep.

Recurrent infection is widespread on Palestinian farms, and it has been suggested that shed scabs may harbor virus for future infection, but this farm was partially decontaminated and there was no rearing of new animals between the two outbreaks. Molecular sequence comparison of the F1L gene from humans and source animals indicated that F1L gene amplicons from humans were identical to those from infected animals in both outbreaks, but there were 24 nucleotides differences between the Palestinian isolates of the first and second outbreak indicating a fresh reintroduction of virus in 2019. Intriguingly, a third outbreak restricted to lamb in 2021 displayed a 99.1% identity with the 2016 outbreak. These results suggest that the 0.9% sequence difference between 2016 and 2021 may be possible from reintroduction of a third virus to the farm, or due to mutation occurring on the first virus that may still be present in the farm.

## CHAPTER (6)

### 6. Conclusion

To the best of our knowledge, this is the first study investigate viral determinants that contribute to ORFV zoonosis. In this work, the use of a comparative genomic approach enabled the identification of the one gene with twelve non-synonymous substitutions that together correlate with ORFV zoonosis or viral propagation in, and adaptation to, cell culture.

Further experiments would be valuable to predict the functional impact of these substitution mutations. Although this study greatly added to the small number of available sequences from zoonotic cases, more samples with full genome sequencing from around the world would be useful, especially to identify additional potential determinants that may be less strongly correlated with zoonosis than those found in this gene.

In addition, this is the first report tackling epidemiological and molecular insights of ORFV circulating in Palestine. The Palestinian zoonoses highlight the ease with which ORFV may transmit from animals to humans, and hence the importance of continued surveillance and analysis of zoonotic events.

## References

- A. Bratkea, McLysaghta, R. (2013). 基因的改变NIH Public Access. *Infection, Genetics and Evolution*, 14(1), 406–425. <https://doi.org/10.1038/jid.2014.371>
- A. Bratkea, McLysaghta, R., Access, O., Andreani, J., Fongue, J., Bou Khalil, J. Y., David, L., Mougari, S., Le Bideau, M., Abrahão, J., Berbis, P., La Scola, B., Boyer, M., Gimenez, G., Suzan-Monti, M., Raoult, D., Cao, J., Varga, J., Deschambault, Y., Chen, D.-Y., ... Stoye, J. (2019). Sheep-to-human transmission of orf virus during eid al-Adha religious practices, France. *Journal of General Virology*, 7(1), 1–5. <https://doi.org/10.3389/fmicb.2015.01135>
- Abdullah, A. A., Ismail, M. F. Bin, Balakrishnan, K. N., Bala, J. A., Hani, H., Abba, Y., Awang Isa, M. K., Abdullah, F. F. J., Arshad, S. S., Nazariah, Z. A., Abdullah, R., Mustapha, N. M., & Mohd-Lila, M.-A. (2015). Isolation and phylogenetic analysis of caprine Orf virus in Malaysia. *Virusdisease*, 26(4), 255–259. <https://doi.org/10.1007/s13337-015-0278-4>
- Ahanger, S. A., Parveen, R., Nazki, S., Dar, Z., Dar, T., Dar, K. H., Dar, A., Rai, N., & Dar, P. (2018). Detection and phylogenetic analysis of Orf virus in Kashmir Himalayas. *VirusDisease*, 29(3), 405–410. <https://doi.org/10.1007/s13337-018-0473-1>
- Alcami, A., & Koszinowski, U. H. (2000). Viral mechanisms of immune evasion. In *Trends in Microbiology* (Vol. 8, Issue 9, pp. 410–418). Elsevier Current Trends. [https://doi.org/10.1016/S0966-842X\(00\)01830-8](https://doi.org/10.1016/S0966-842X(00)01830-8)
- Andreani, J., Fongue, J., Bou Khalil, J. Y., David, L., Mougari, S., Le Bideau, M., Abrahão, J., Berbis, P., & La Scola, B. (2019). Human infection with ORF virus and description of its whole genome, France, 2017. *Emerging Infectious Diseases*, 25(12), 2197–2204. <https://doi.org/10.3201/eid2512.181513>
- Azwai, S. M., Carter, S. D., & Woldehiwet, Z. (1995). Immune responses of the camel (*Camelus dromedarius*) to contagious ecthyma (orf) virus infection. *Veterinary Microbiology*, 47(1–2). [https://doi.org/10.1016/0378-1135\(95\)00055-F](https://doi.org/10.1016/0378-1135(95)00055-F)
- Bala, J. A., Balakrishnan, K. N., Abdullah, A. A., Adamu, L., Noorzahari, M. S. bin, May, L. K., Mangga, H. K., Ghazali, M. T., Mohamed, R. Bin, Haron, A. W., Noordin, M. M., & Lila, M. A. M. (2019). An association of Orf virus infection among sheep and goats with herd health programme in Terengganu state, eastern region of the peninsular Malaysia. *BMC Veterinary Research*, 15(1), 250. <https://doi.org/10.1186/s12917-019-1999-1>
- Bala, J. A., Balakrishnan, K. N., Abdullah, A. A., Mohamed, R., Haron, A. W., Jesse, F. F. A.,

- Noordin, M. M., & Mohd-Azmi, M. L. (2018). The re-emerging of orf virus infection: A call for surveillance, vaccination and effective control measures. In *Microbial Pathogenesis* (Vol. 120, pp. 55–63). Academic Press. <https://doi.org/10.1016/j.micpath.2018.04.057>
- Ballanger, F., Barbarot, S., Mollat, C., Bossard, C., Cassagnau, E., Renac, F., & Stalder, J. F. (2006). Two giant orf lesions in a heart/lung transplant patient. *European Journal of Dermatology : EJD*, 16(3), 284–286.
- Barrett, J. W., & McFadden, G. (2008). Origin and Evolution of Poxviruses. In *Origin and Evolution of Viruses* (Second Edi). Elsevier Ltd. <https://doi.org/10.1016/B978-0-12-374153-0.00019-9>
- Bergqvist, C., Kurban, M., & Abbas, O. (2017). Orf virus infection. *Reviews in Medical Virology*, 27(4), 1–9. <https://doi.org/10.1002/rmv.1932>
- Bouscarat, F., & Descamps, V. (2017). Wife to husband transmission of Ecthyma contagiosum (Orf). *IDCases*, 9, 28–29. <https://doi.org/10.1016/j.idcr.2017.05.007>
- Chi, X., Zeng, X., Hao, W., Li, M., & Li, W. (2013). Heterogeneity among Orf Virus Isolates from Goats in Fujian Province, Southern China. *PLoS ONE*, 8(10). <https://doi.org/10.1371/journal.pone.0066958>
- Couñago, R. M., Knapp, K. M., Nakatani, Y., Fleming, S. B., Corbett, M., Wise, L. M., Mercer, A. A., & Krause, K. L. (2015). Structures of Orf Virus Chemokine Binding Protein in Complex with Host Chemokines Reveal Clues to Broad Binding Specificity. *Structure*, 23(7), 1199–1213. <https://doi.org/10.1016/j.str.2015.04.023>
- Crooks, G. E., Hon, G., Chandonia, J.-M., & Brenner, S. E. (2004). WebLogo: A Sequence Logo Generator. *Genome Res*, 14, 1188–1190. <https://doi.org/10.1101/gr.849004>
- Delhon, G., Tulman, E. R., Afonso, C. L., Lu, Z., de la Concha-Bermejillo, A., Lehmkuhl, H. D., Piccone, M. E., Kutish, G. F., & Rock, D. L. (2004). Genomes of the Parapoxviruses Orf Virus and Bovine Papular Stomatitis Virus. *Journal of Virology*, 78(1), 168–177. <https://doi.org/10.1128/jvi.78.1.168-177.2004>
- Dill, V., Hoffmann, B., Zimmer, A., Beer, M., & Eschbaumer, M. (2018). Influence of cell type and cell culture media on the propagation of foot-and-mouth disease virus with regard to vaccine quality. *Virology Journal*, 15(1), 46. <https://doi.org/10.1186/s12985-018-0956-0>
- Duchateau, N. C., Aerts, O., & Lambert, J. (2014). Autoinoculation with Orf virus (ecthyma contagiosum). *International Journal of Dermatology*, 53(1), e60–e62.

<https://doi.org/https://doi.org/10.1111/j.1365-4632.2012.05622.x>

Engel, P., & Angulo, A. (2012). Viral immunomodulatory proteins: usurping host genes as a survival strategy. *Advances in Experimental Medicine and Biology*, 738, 256–276.

[https://doi.org/10.1007/978-1-4614-1680-7\\_15](https://doi.org/10.1007/978-1-4614-1680-7_15)

Fairley, R. A., Whelan, E. M., Pesavento, P. A., & Mercer, A. A. (2008). Recurrent localised cutaneous parapoxvirus infection in three cats. *New Zealand Veterinary Journal*, 56(4).

<https://doi.org/10.1080/00480169.2008.36833>

Felix, J., Kandiah, E., De Munck, S., Bloch, Y., Van Zundert, G. C. P., Pauwels, K., Dansercoer, A., Novanska, K., Read, R. J., Bonvin, A. M. J. J., Vergauwen, B., Verstraete, K., Gutsche, I., & Savvides, S. N. (2016). Structural basis of GM-CSF and IL-2 sequestration by the viral decoy receptor GIF. *Nature Communications*, 7, 1–13.

<https://doi.org/10.1038/ncomms13228>

Fla', F., Da Fonseca, F. G., Wolffe, E. J., Weisberg, A., & Moss, B. (2000). Characterization of the Vaccinia Virus H3L Envelope Protein: Topology and Posttranslational Membrane Insertion via the C-Terminal Hydrophobic Tail. In *JOURNAL OF VIROLOGY* (Vol. 74, Issue 16). <http://jvi.asm.org/>

Fleming, S. B., McCaughan, C., Lateef, Z., Dunn, A., Wise, L. M., Real, N. C., & Mercer, A. A. (2017). Deletion of the chemokine binding protein gene from the parapoxvirus ORF virus reduces virulence and pathogenesis in sheep. *Frontiers in Microbiology*, 8(JAN), 1–17.

<https://doi.org/10.3389/fmicb.2017.00046>

Fleming, S. B., & Mercer, A. A. (2007). Genus Parapoxvirus. In *Poxviruses* (pp. 127–165). Birkhäuser Basel. [https://doi.org/10.1007/978-3-7643-7557-7\\_7](https://doi.org/10.1007/978-3-7643-7557-7_7)

Fleming, S. B., Wise, L. M., & Mercer, A. A. (2015). Molecular genetic analysis of orf virus: A poxvirus that has adapted to skin. *Viruses*, 7(3), 1505–1539.

<https://doi.org/10.3390/v7031505>

Frandsen, J., Enslow, M., & Bowen, A. R. (2011). Orf parapoxvirus infection from a cat scratch. *Dermatology Online Journal*, 17(4).

Gill, M. J., Arlette, J., Buchan, K. A., & Barber, K. (1990). Human orf. A diagnostic consideration? *Archives of Dermatology*, 126(3), 356–358.

González-Motos, V., Kropp, K. A., & Viejo-Borbolla, A. (2016). Chemokine binding proteins: An immunomodulatory strategy going viral. *Cytokine and Growth Factor Reviews*,

30(2015), 71–80. <https://doi.org/10.1016/j.cytogfr.2016.02.007>

Guo, J., Rasmussen, J., Wünschmann, A., & De La Concha-Bermejillo, A. (2004). Genetic characterization of orf viruses isolated from various ruminant species of a zoo. *Veterinary Microbiology*, 99(2). <https://doi.org/10.1016/j.vetmic.2003.11.010>

Haig, D. (2006). Orf virus infection and host immunity. *Current Opinion in Infectious Diseases*, 19, 127–131. <https://doi.org/10.1097/01.qco.0000216622.75326.ef>

Haig, D. M. K., McInnes, C., Deane, D., Reid, H., & Mercer, A. (1997). The immune and inflammatory response to ORF virus. *Comparative Immunology, Microbiology and Infectious Diseases*, 20(3), 197–204. [https://doi.org/10.1016/S0147-9571\(96\)00045-8](https://doi.org/10.1016/S0147-9571(96)00045-8)

Heare, D., Little, S., Weise, D., Harris, J., Hillhouse, A., Konganti, K., & Lawhon, S. (2020). Whole-Genome Sequence of an Orf Virus Isolate Derived from a Cell Culture Infected with Contagious Ecthyma Vaccine. *Microbiology Resource Announcements*, 9. <https://doi.org/10.1128/MRA.00752-20>

Hosamani, M., Scagliarini, A., Bhanuprakash, V., McInnes, C. J., & Singh, R. K. (2009). Orf: An update on current research and future perspectives. *Expert Review of Anti-Infective Therapy*, 7(7), 879–893. <https://doi.org/10.1586/ERI.09.64>

Housawi, F. M. T., Roberts, G. M., Gilray, J. A., Pow, I., Reid, H. W., Nettleton, P. F., Sumption, K. J., Hibma, M. H., & Mercer, A. A. (1998). The reactivity of monoclonal antibodies against off virus with other parapoxviruses and the identification of a 39 kDa immunodominant protein. *Archives of Virology*, 143(12), 2289–2303. <https://doi.org/10.1007/s007050050461>

Hughes, C. E., & Nibbs, R. J. B. (2018). A guide to chemokines and their receptors. *The FEBS Journal*, 285(16), 2944–2971. <https://doi.org/10.1111/febs.14466>

Ichihashi, Y. (1996). Extracellular enveloped vaccinia virus escapes neutralization. *Virology*, 217(2), 478–485. <https://doi.org/10.1006/viro.1996.0142>

James, N. (2017). Poxviridae. In *Fenner's veterinary virology* (Fifth Edit, pp. 157–174). Elsevier Academic Press. <https://doi.org/10.1016/B978-0-12-800946-8.00007-6>

Johnston, J. B., & McFadden, G. (2003). Poxvirus immunomodulatory strategies: current perspectives. *Journal of Virology*, 77(11), 6093–6100. <https://doi.org/10.1128/jvi.77.11.6093-6100.2003>

Kassa, T. (2021). *A Review on Human Orf: A Neglected Viral Zoonosis*.

<https://doi.org/10.2147/RRTM.S306446>

Kennedy, C. T. C., & Lyell, A. (1984). Perianal orf. *Journal of the American Academy of Dermatology*, 11(1), 72–74. [https://doi.org/10.1016/S0190-9622\(84\)70137-X](https://doi.org/10.1016/S0190-9622(84)70137-X)

Kumar, R., Trivedi, R. N., Bhatt, P., Khan, S. U. H., Khurana, S. K., Tiwari, R., Karthik, K., Malik, Y. S., Dhama, K., & Chandra, R. (2015). Contagious Pustular Dermatitis (Orf Disease) - Epidemiology, Diagnosis, Control and Public Health Concerns. *Advances in Animal and Veterinary Sciences*, 3(12).

<https://doi.org/10.14737/journal.aavs/2015/3.12.649.676>

Kumar, S., Stecher, G., Li, M., Knyaz, C., & Tamura, K. (2018). MEGA X: Molecular evolutionary genetics analysis across computing platforms. *Molecular Biology and Evolution*, 35(6), 1547–1549. <https://doi.org/10.1093/molbev/msy096>

Kummeneje, K., & Krogsrud, J. (1979). Contagious ecthyma (orf) in reindeer (*Rangifer tarandus*). *The Veterinary Record*, 105(3). <https://doi.org/10.1136/vr.105.3.60>

Lalani, A. S., & McFadden, G. (1997). Secreted poxvirus chemokine binding proteins. In *Journal of Leukocyte Biology* (Vol. 62, Issue 5, pp. 570–576).

<https://doi.org/10.1002/jlb.62.5.570>

Lateef, Z., Baird, M. A., Wise, L. M., Young, S., Mercer, A. A., & Fleming, S. B. (2010). The chemokine-binding protein encoded by the poxvirus orf virus inhibits recruitment of dendritic cells to sites of skin inflammation and migration to peripheral lymph nodes.

*Cellular Microbiology*, 12(5), 665–676. <https://doi.org/10.1111/j.1462-5822.2009.01425.x>

Lederman, E. R., Green, G. M., DeGroot, H. E., Dahl, P., Goldman, E., Greer, P. W., Li, Y., Zhao, H., Paddock, C. D., & Damon, I. K. (2007). Progressive Orf Virus Infection in a Patient with Lymphoma: Successful Treatment Using Imiquimod. *Clinical Infectious Diseases*, 44(11), e100–e103. <https://doi.org/10.1086/517509>

Li, W., Hao, W., Peng, Y., Duan, C., Tong, C., Song, D., Gao, F., Li, M., Rock, D. L., & Luo, S. (2015). Comparative genomic sequence analysis of Chinese orf virus strain NA1/11 with other parapoxviruses. *Archives of Virology*, 160(1), 253–266.

<https://doi.org/10.1007/s00705-014-2274-1>

Li, W., Ning, Z., Hao, W., Song, D., Gao, F., Zhao, K., Liao, X., Li, M., Rock, D. L., & Luo, S. (2012). Isolation and phylogenetic analysis of orf virus from the sheep herd outbreak in northeast China. *BMC Veterinary Research*, 8(1), 1. <https://doi.org/10.1186/1746-6148-8->

- Lin, C.-L., Chung, C.-S., Heine, H. G., & Chang, W. (2000). Vaccinia Virus Envelope H3L Protein Binds to Cell Surface Heparan Sulfate and Is Important for Intracellular Mature Virion Morphogenesis and Virus Infection In Vitro and In Vivo. In *JOURNAL OF VIROLOGY* (Vol. 74, Issue 7). <http://jvi.asm.org/>
- Luster, A. D. (1998). Chemokines--chemotactic cytokines that mediate inflammation. *The New England Journal of Medicine*, 338(7), 436–445.  
<https://doi.org/10.1056/NEJM199802123380706>
- Manley, F. H. (1934). Observations on the Virus of Contagious Pustular Dermatitis. *The Veterinary Journal (1900)*, 90(2), 80–92. [https://doi.org/https://doi.org/10.1016/S0372-5545\(17\)38813-2](https://doi.org/https://doi.org/10.1016/S0372-5545(17)38813-2)
- Midilli, K., Erkılıç, A., Kuşucu, M., Analay, H., Erkılıç, S., Benzonana, N., Yıldırım, M. S., Mülâyim, K., Acar, H., & Ergonul, O. (2013). Nosocomial outbreak of disseminated orf infection in a burn unit, Gaziantep, Turkey, October to December 2012. *Eurosurveillance*, 18(11), 20425.
- Moss, B. (2012). *Poxvirus Cell Entry: How Many Proteins Does it Take?* 688–707.  
<https://doi.org/10.3390/v4050688>
- Moss, B. (2013). Poxvirus DNA Replication. *Cold Spring Harb Perspect Biol*, 5(9)(a010199), 1–12. <https://doi.org/10.1101/cshperspect.a010199>
- Moss, B., & Shisler, J. L. (2001). Immunology 101 at poxvirus U: Immune evasion genes. *Seminars in Immunology*, 13(1), 59–66. <https://doi.org/10.1006/SMIM.2000.0296>
- Muhsen, M., Protschka, M., Schneider, L. E., Müller, U., Köhler, G., Magin, T. M., Büttner, M., Alber, G., & Siegemund, S. (2019). Orf virus (ORFV) infection in a three-dimensional human skin model: Characteristic cellular alterations and interference with keratinocyte differentiation. *PLoS ONE*, 14(1), 1–22. <https://doi.org/10.1371/journal.pone.0210504>
- Nandi, S., De, U. K., & Chowdhury, S. (2011). Current status of contagious ecthyma or orf disease in goat and sheep-A global perspective. In *Small Ruminant Research* (Vol. 96, Issues 2–3, pp. 73–82). Elsevier. <https://doi.org/10.1016/j.smallrumres.2010.11.018>
- Newsom, I. E., & Cross, F. (1934). Sore Mouth in Sheep Transmissible to Man. *Journal of the American Veterinary Medical Association*, 84, 799–802.
- Nougairede, A., Fossati, C., Salez, N., Cohen-Bacrie, S., Ninove, L., Michel, F., Aboukais, S.,



Buttner, M., Zandotti, C., de Lamballerie, X., & Charrel, R. N. (2013). Sheep-to-human transmission of orf virus during eid al-Adha religious practices, France. *Emerging Infectious Diseases*, 19(1), 102–105. <https://doi.org/10.3201/eid1901.120421>

Page, A. J., Cummins, C. A., Hunt, M., Wong, V. K., Reuter, S., Holden, M. T. G., Fookes, M., Falush, D., Keane, J. A., & Parkhill, J. (2015). Roary: Rapid large-scale prokaryote pan genome analysis. *Bioinformatics*, 31(22), 3691–3693. <https://doi.org/10.1093/bioinformatics/btv421>

Portillo, A. Del, Tripodi, J., Najfeld, V., Wodarz, D., Levy, D. N., & Chen, B. K. (2011). Multiploid Inheritance of HIV-1 during Cell-to-Cell Infection. *Journal of Virology*, 85(14), 7169–7176. <https://doi.org/10.1128/JVI.00231-11>

Rajkomar, V., Hannah, M., Coulson, I. H., & Owen, C. M. (2016). A case of human to human transmission of orf between mother and child. *Clinical and Experimental Dermatology*, 41(1), 60–63.

Robinson, A. J., Barns, G., Fraser, K., Carpenter, E., & Mercer, A. A. (1987). Conservation and variation in orf virus genomes. *Virology*, 157(1), 13–23. [https://doi.org/https://doi.org/10.1016/0042-6822\(87\)90308-4](https://doi.org/https://doi.org/10.1016/0042-6822(87)90308-4)

Robinson, A. J., & Mercer, A. A. (1995). Parapoxvirus of Red Deer: Evidence for Its Inclusion as a New Member in the Genus Parapoxvirus. *Virology*, 208(2). <https://doi.org/10.1006/viro.1995.1217>

Rollins, B. J. (1997). Chemokines. In *Blood* (Vol. 90, Issue 3, pp. 909–928). American Society of Hematology. <https://doi.org/10.1182/blood.v90.3.909>

Rørdam, O. M., Grimstad, Ø., Spigset, O., & Ryggen, K. (2013). Giant orf with prolonged recovery in a patient with psoriatic arthritis treated with etanercept. *Acta Dermato-Venereologica*, 93(4), 487–488.

Rot, A., & Von Andrian, U. H. (2004). Chemokines in innate and adaptive host defense: Basic chemokinese grammar for immune cells. *Annual Review of Immunology*, 22, 891–928. <https://doi.org/10.1146/annurev.immunol.22.012703.104543>

Scagliarini, A., Ciulli, S., Battilani, M., Jacoboni, I., Montesi, F., Casadio, R., & Prosperi, S. (2002). Characterisation of immunodominant protein encoded by the F1L gene of orf virus strains isolated in Italy. *Archives of Virology*, 147(10), 1989–1995. <https://doi.org/10.1007/s00705-002-0850-2>

- Scagliarini, A., Gallina, L., Dal Pozzo, F., Battilani, M., Ciulli, S., & Prosperi, S. (2004). Heparin binding activity of orf virus F1L protein. *Virus Research*, 105(2), 107–112. <https://doi.org/10.1016/j.virusres.2004.04.018>
- Schmid, M., Speiseder, T., Dobner, T., & Gonzalez, R. A. (2014). *DNA Virus Replication Compartments*. <https://doi.org/10.1128/JVI.02046-13>
- Seet, B. T., McCaughan, C. A., Handel, T. M., Mercer, A., Brunetti, C., McFadden, G., & Fleming, S. B. (2003). Analysis of an orf virus chemokine-binding protein: Shifting ligand specificities among a family of poxvirus viroceptors. *Proceedings of the National Academy of Sciences of the United States of America*, 100(25), 15137–15142. <https://doi.org/10.1073/pnas.2336648100>
- Sharma, A. K., Venkatesan, G., Mathesh, K., Ram, H., Ramakrishnan, M. A., & Pandey, A. B. (2016). Occurrence and identification of contagious ecthyma in blackbuck. *VirusDisease*, 27(2). <https://doi.org/10.1007/s13337-016-0316-x>
- Sharp, P. M., & Simmonds, P. (2011). Evaluating the evidence for virus/host co-evolution. In *Current Opinion in Virology* (Vol. 1, Issue 5, pp. 436–441). Elsevier B.V. <https://doi.org/10.1016/j.coviro.2011.10.018>
- Smith, G. L., Vanderplassen, A., & Law, M. (2002). The formation and function of extracellular enveloped vaccinia virus. *Journal of General Virology*, 83(12), 2915–2931. <https://doi.org/10.1099/0022-1317-83-12-2915>
- Spehner, D., De Carlo, S., Drillien, R., Weiland, F., Mildner, K., Hanau, D., & Rziha, H.-J. (2004). Appearance of the Bona Fide Spiral Tubule of Orf Virus Is Dependent on an Intact 10-Kilodalton Viral Protein. *Journal of Virology*, 78(15), 8085–8093. <https://doi.org/10.1128/jvi.78.15.8085-8093.2004>
- Spyrou, V., & Valiakos, G. (2015). Orf virus infection in sheep or goats. *Veterinary Microbiology*, 181(1–2), 178–182. <https://doi.org/10.1016/j.vetmic.2015.08.010>
- Stead, J. W., Henry, C. M., & Simpson, R. H. (1992). Rare case of autoinoculation of orf. *The British Journal of General Practice : The Journal of the Royal College of General Practitioners*, 42(362), 395–396. <https://pubmed.ncbi.nlm.nih.gov/1457180>
- Stewart, A. C. (1983). Epidemiology of orf. *The New Zealand Medical Journal*, 96(725), 100–101.
- Stone, M. J., Hayward, J. A., Huang, C., E Huma, Z., & Sanchez, J. (2017). Mechanisms of

- Regulation of the Chemokine-Receptor Network. *International Journal of Molecular Sciences*, 18(2), 342. <https://doi.org/10.3390/ijms18020342>
- Tan, J. L., Ueda, N., Mercer, A. A., & Fleming, S. B. (2009). Investigation of orf virus structure and morphogenesis using recombinants expressing FLAG-tagged envelope structural proteins: Evidence for wrapped virus particles and egress from infected cells. *Journal of General Virology*, 90(3), 614–625. <https://doi.org/10.1099/vir.0.005488-0>
- Tan, S. T., Blake, G. B., & Chambers, S. (1991). Recurrent orf in an immunocompromised host. *British Journal of Plastic Surgery*, 44(6), 465–467. [https://doi.org/10.1016/0007-1226\(91\)90209-3](https://doi.org/10.1016/0007-1226(91)90209-3)
- Tedla, M., Berhan, N., Molla, W., Temesgen, W., & Alemu, S. (2018). Molecular identification and investigations of contagious ecthyma (Orf virus) in small ruminants, North west Ethiopia. *BMC Veterinary Research*, 14(1), 13. <https://doi.org/10.1186/s12917-018-1339-x>
- Thomas, K., Tompkins, D. M., Sainsbury, A. W., Wood, A. R., Dalziel, R., Nettleton, P. F., & McInnes, C. J. (2003). A novel poxvirus lethal to red squirrels (*Sciurus vulgaris*). *Journal of General Virology*, 84(12). <https://doi.org/10.1099/vir.0.19464-0>
- Tryland, M., Klein, J., Nordøy, E. S., & Blix, A. S. (2005). Isolation and partial characterization of a parapoxvirus isolated from a skin lesion of a Weddell seal. *Virus Research*, 108(1–2). <https://doi.org/10.1016/j.virusres.2004.08.005>
- Turk, B., Senturk, B., Dereli, T., & Yaman, B. (2013). A rare human-to-human transmission of orf. *International Journal of Dermatology*, 53(1), 63–65. doi:10.1111/j.1365-4632.2012.05669.x
- Uzel, M., Samsa, S., Bakris, S., Cetinus, E., Bilgic, E., Karaoguz, A., Ozkul, A., & Arican, O. (2005). A viral infection of the hand commonly seen after the feast of sacrifice : human orf ( orf of the hand ). *Epidemiol Infect*, 133(4), 653–657. 10.1017/s0950268805003778
- Wang, R., & Luo, S. (2018). Orf Virus: A New Class of Immunotherapy Drugs. In *Systems Biology*. IntechOpen.
- Westphal, H. O. (1973). Human to human transmission of orf. *Cutis*, 11, 203–205.
- Yang, H., Meng, Q., Qiao, J., Peng, Y., Xie, K., Liu, Y., Zhao, H., Cai, X., & Chen, C. (2014). Detection of genetic variations in Orf virus isolates epidemic in Xinjiang China. *Journal of Basic Microbiology*, 54(11), 1273–1278. <https://doi.org/10.1002/jobm.201300911>
- Yogisharadhya, R., Bhanuprakash, V., Kumar, A., Mondal, M., & Shivachandra, S. B. (2018).

Comparative sequence and structural analysis of Indian orf viruses based on major envelope immuno-dominant protein (F1L), an homologue of pox viral p35/H3 protein. *Gene*, 663(2017), 72–82. <https://doi.org/10.1016/j.gene.2018.04.026>

Zeedan, G. S. (2015). Isolation and Molecular Diagnosis of Orf Virus from Small Ruminants and Human in Egypt. *Journal of Antivirals & Antiretrovirals*, 07(01), 2–9. <https://doi.org/10.4172/jaa.1000113>

## Supplementary data

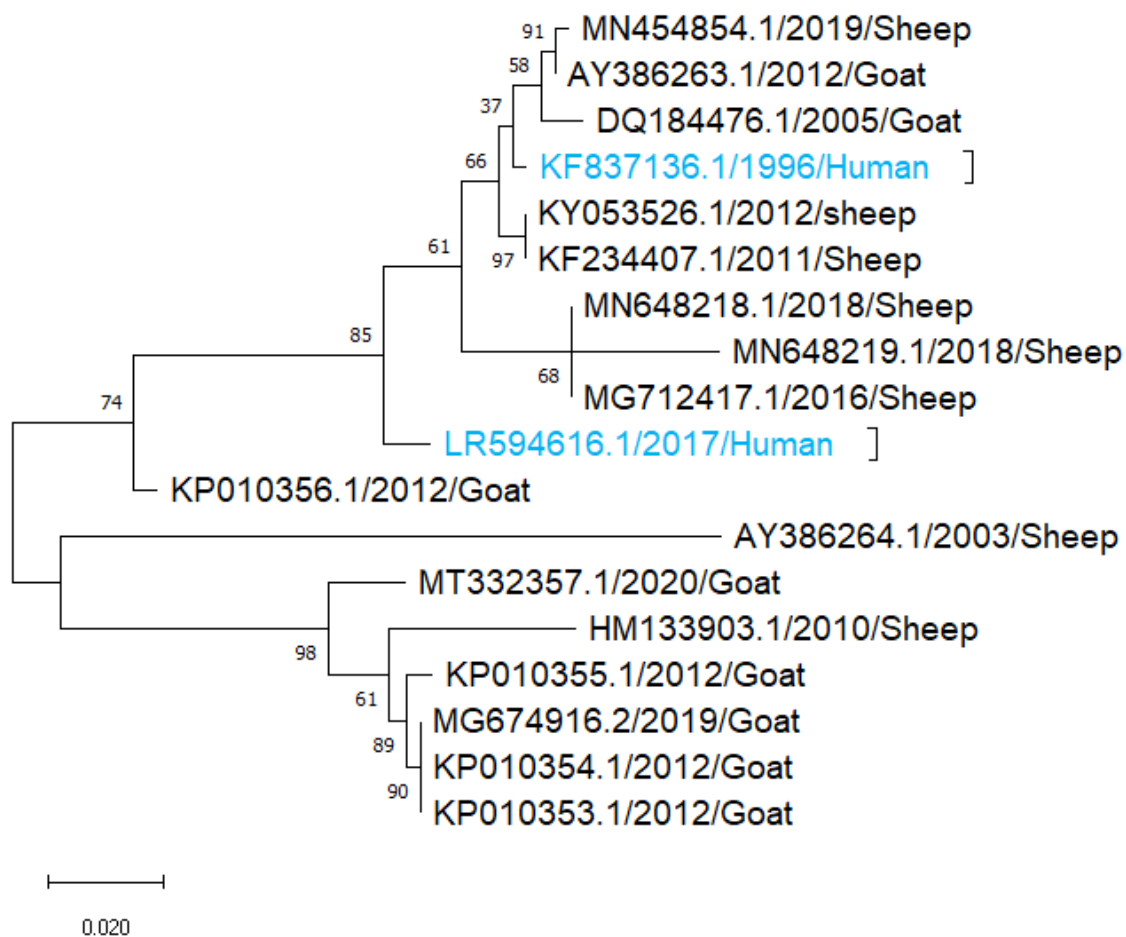


**Figure S.1: Phylogenetic analysis based on ORF001 nucleotide sequences.** Maximum likelihood method was used for analysis with a bootstrap test (1000 replicate). The tree is drawn to scale, with

branch lengths in the same units as those of the evolutionary distances used to infer the phylogenetic tree. The human derived ORFV isolates are highlighted in blue.

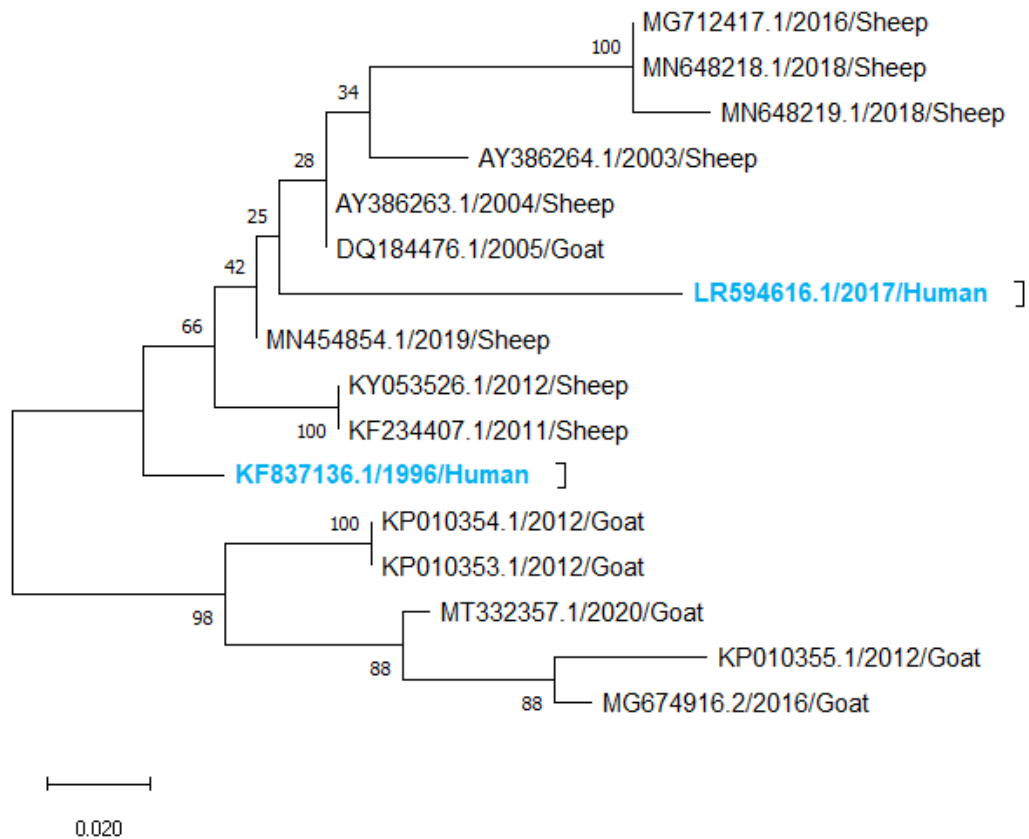


**Figure S.2: Phylogenetic analysis based on ORF005 nucleotide sequences.** Maximum likelihood method was used for analysis with a bootstrap test (1000 replicate). The tree is drawn to scale, with branch lengths in the same units as those of the evolutionary distances used to infer the phylogenetic tree. The human derived ORFV isolates are highlighted in blue.

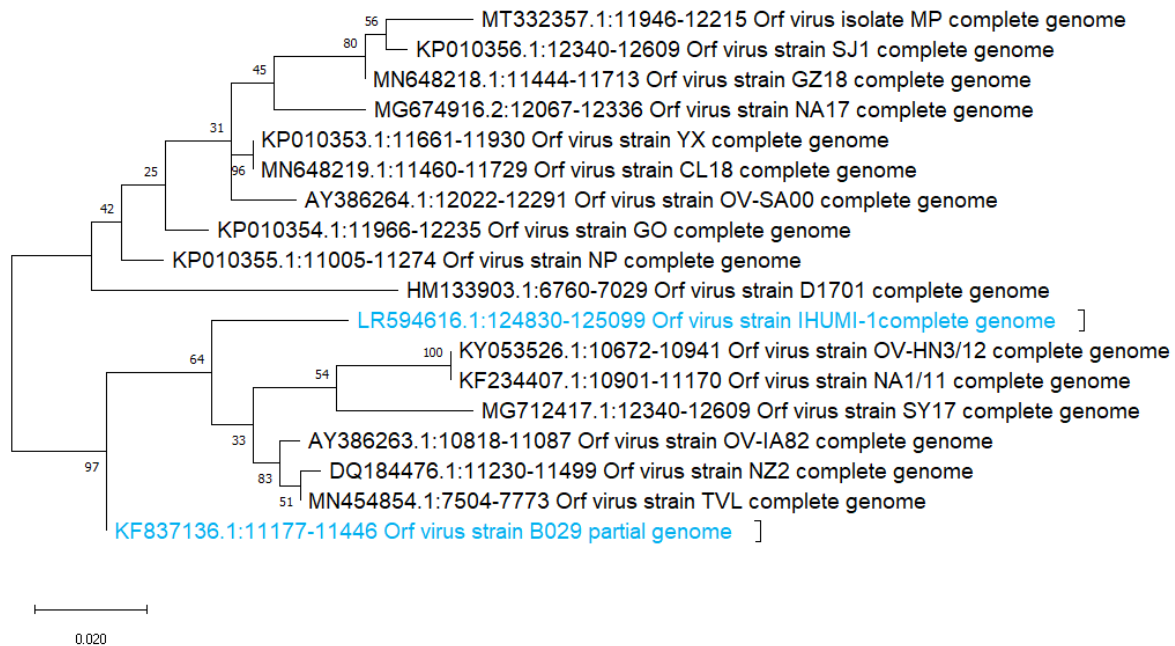


**Figure S.3: Phylogenetic analysis based on ORF012 nucleotide sequences.** Maximum likelihood method was used for analysis with a bootstrap test (1000 replicate). The tree is drawn to scale, with branch lengths in the same units as those of the evolutionary distances used to infer the phylogenetic tree. The human derived ORFV isolates are highlighted in blue.

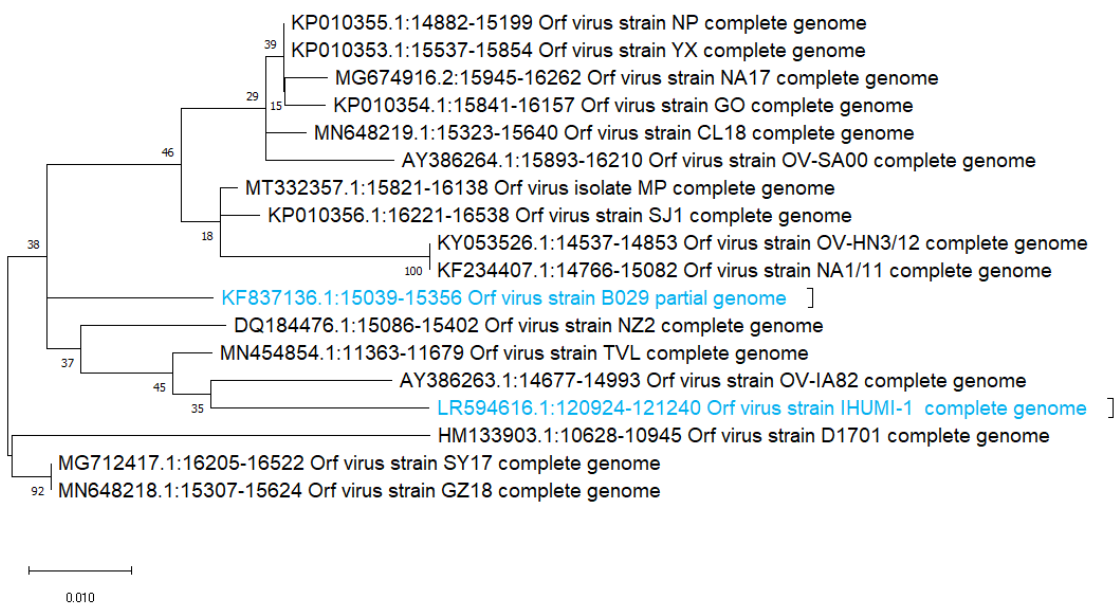


**Figure S.4: Phylogenetic analysis based on ORF017 nucleotide sequences.** Maximum likelihood method was used for analysis with a bootstrap test (1000 replicate). The tree is drawn to scale, with branch lengths in the same units as those of the evolutionary distances used to infer the phylogenetic tree. The human derived ORFV isolates are highlighted in blue.

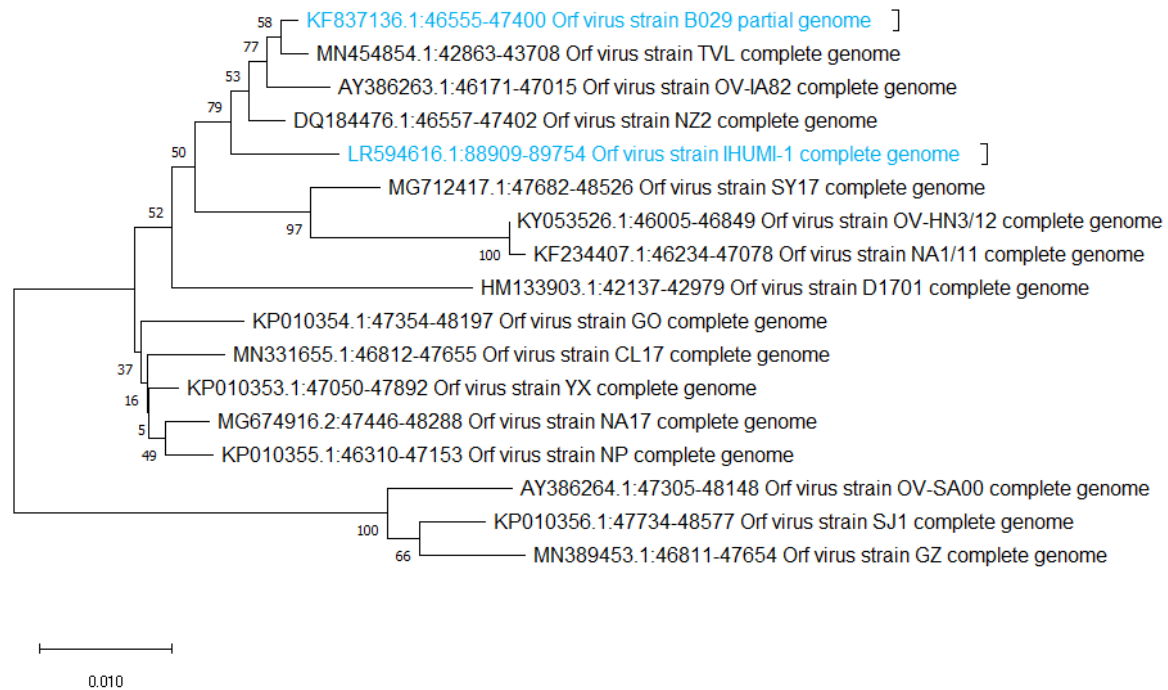


**Figure S.5: Phylogenetic analysis based on ORF 046 nucleotide sequences.** Maximum likelihood method was used for analysis with a bootstrap test (1000 replicate). The tree is drawn to scale, with branch lengths in the same units as those of the evolutionary distances used to infer the phylogenetic tree. The human derived ORFV isolates are highlighted in blue

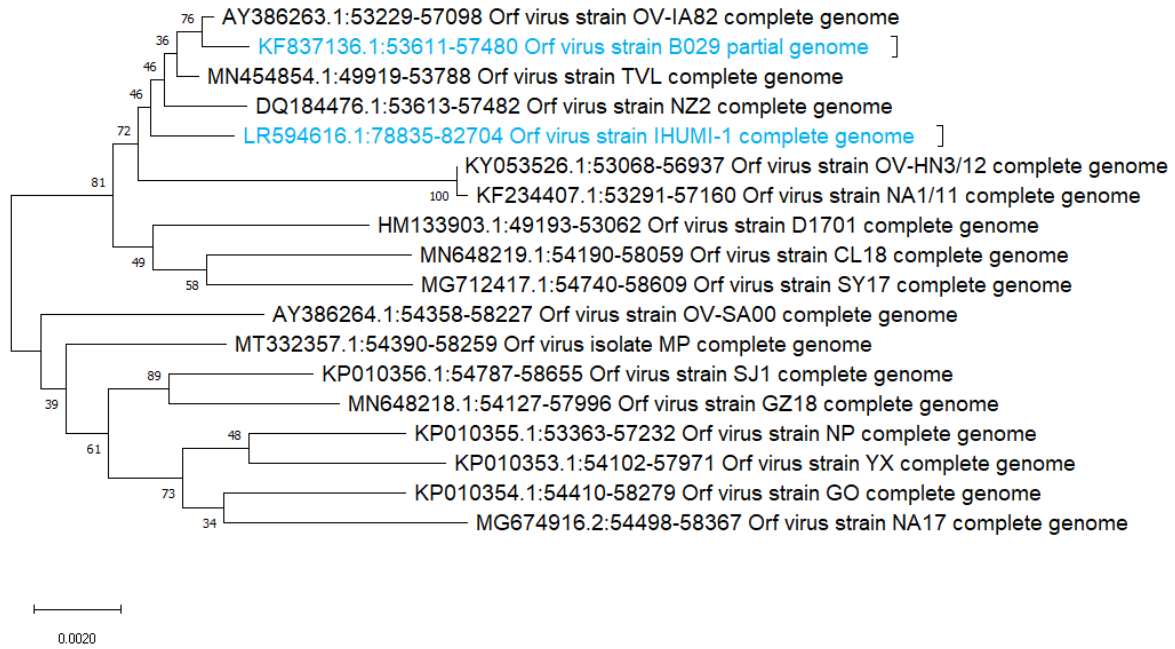


**Figure S.6: Phylogenetic analysis based on ORF056 nucleotide sequences.** Maximum likelihood method was used for analysis with a bootstrap test (1000 replicate). The tree is drawn to scale, with branch lengths in the same units as those of the evolutionary distances used to infer the phylogenetic tree. The human derived ORFV isolates are highlighted in blue.



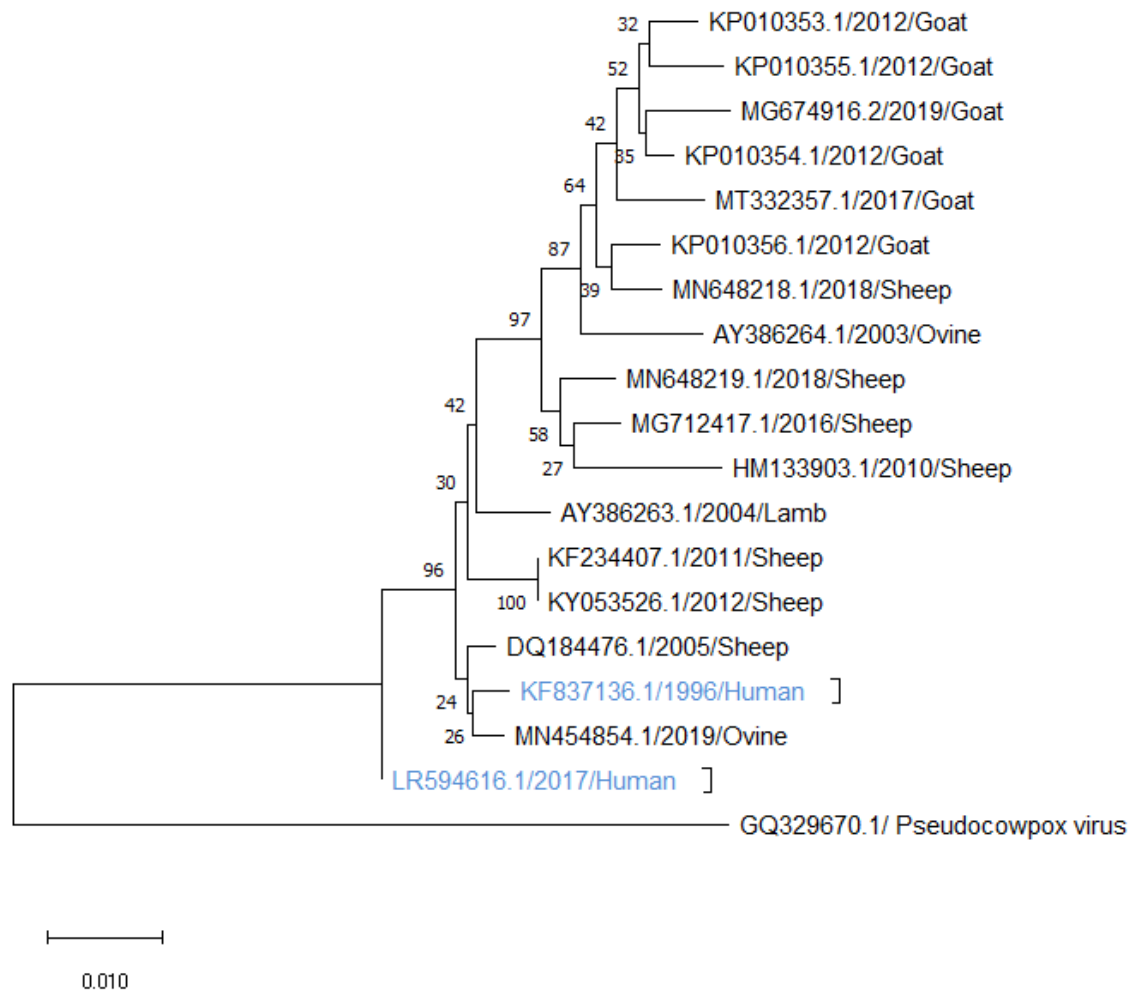


**Figure S.7: Phylogenetic analysis based on ORF059 nucleotide sequences.** Maximum likelihood method was used for analysis with a bootstrap test (1000 replicate). The tree is drawn to scale, with branch lengths in the same units as those of the evolutionary distances used to infer the phylogenetic tree. The human derived ORFV isolates are highlighted in blue

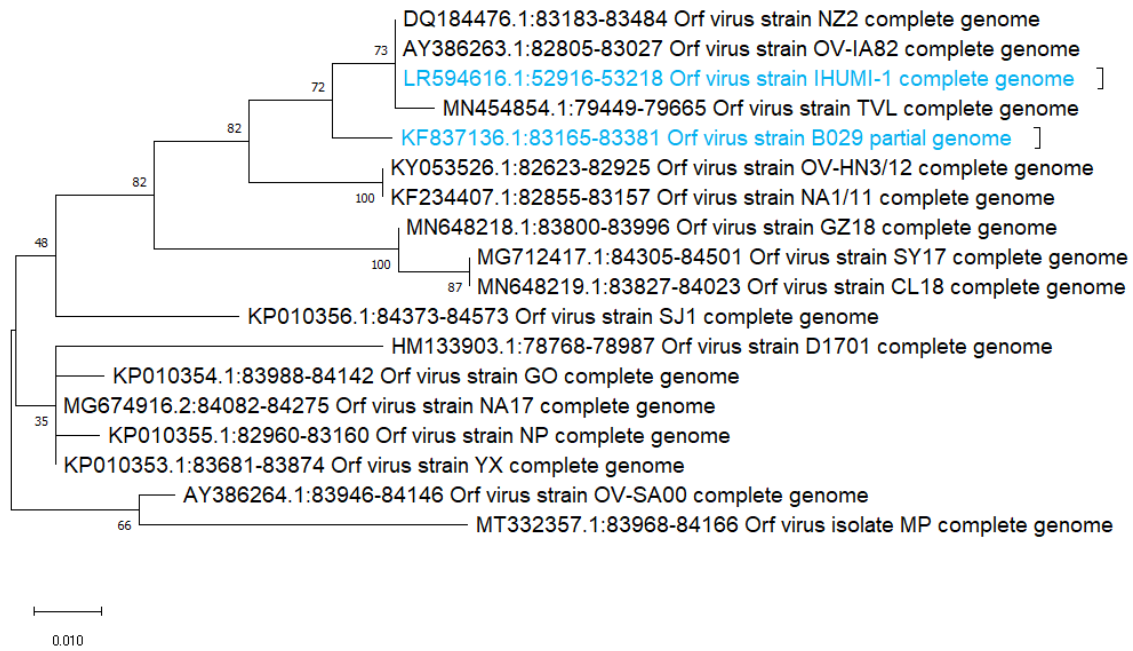


**Figure S.8: Phylogenetic analysis based on ORF080 nucleotide sequences.** Maximum likelihood method was used for analysis with a bootstrap test (1000 replicate). The tree is drawn to scale, with branch lengths in the same units as those of the evolutionary distances used to infer the phylogenetic tree. The human derived ORFV isolates are highlighted in blue.

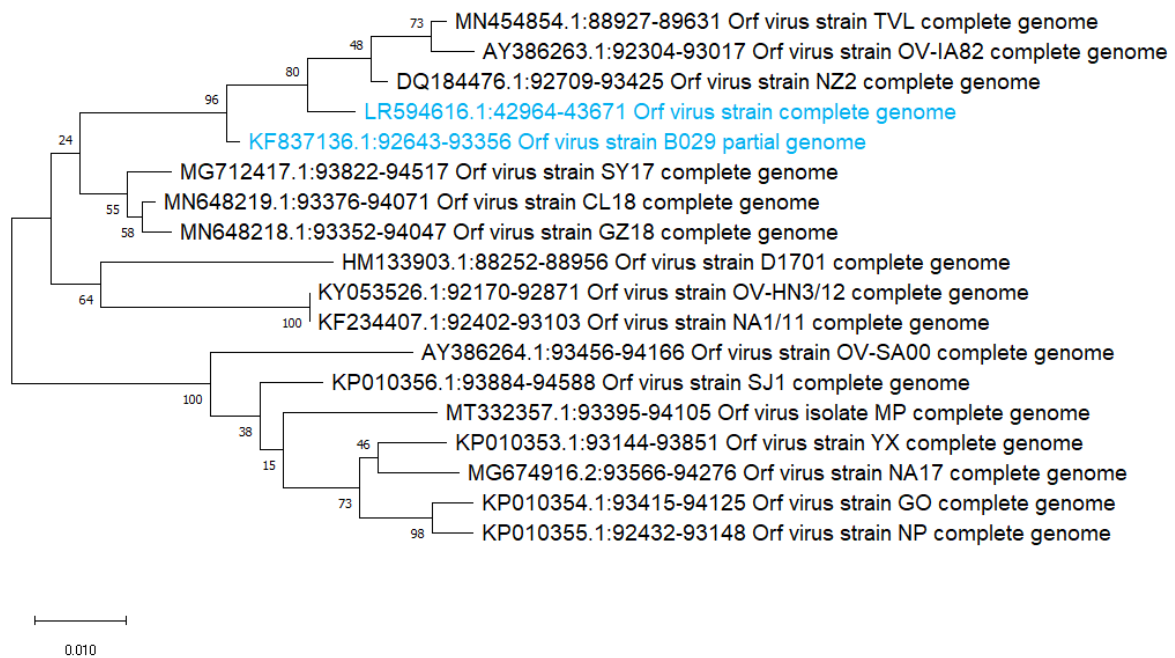


**Figure S.9: Phylogenetic analysis based on ORF088 nucleotide sequences.** Maximum likelihood method was used for analysis with a bootstrap test (1000 replicate). The tree is drawn to scale, with branch lengths in the same units as those of the evolutionary distances used to infer the phylogenetic tree. The human derived ORFV isolates are highlighted in blue.

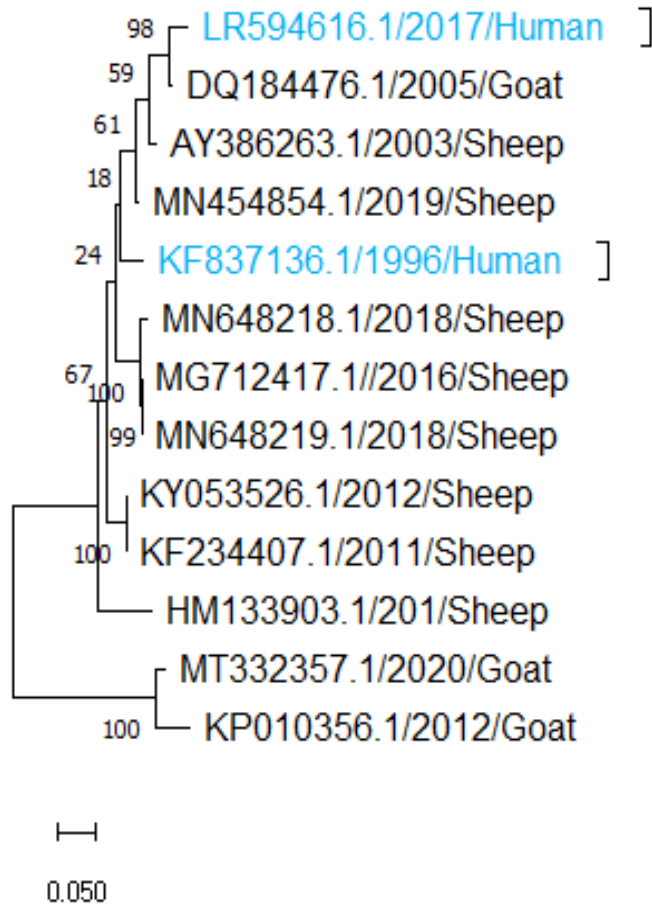


**Figure S.10: Phylogenetic analysis based on ORF116 nucleotide sequences.** Maximum likelihood method was used for analysis with a bootstrap test (1000 replicate). The tree is drawn to scale, with branch lengths in the same units as those of the evolutionary distances used to infer the phylogenetic tree. The human derived ORFV isolates are highlighted in blue.

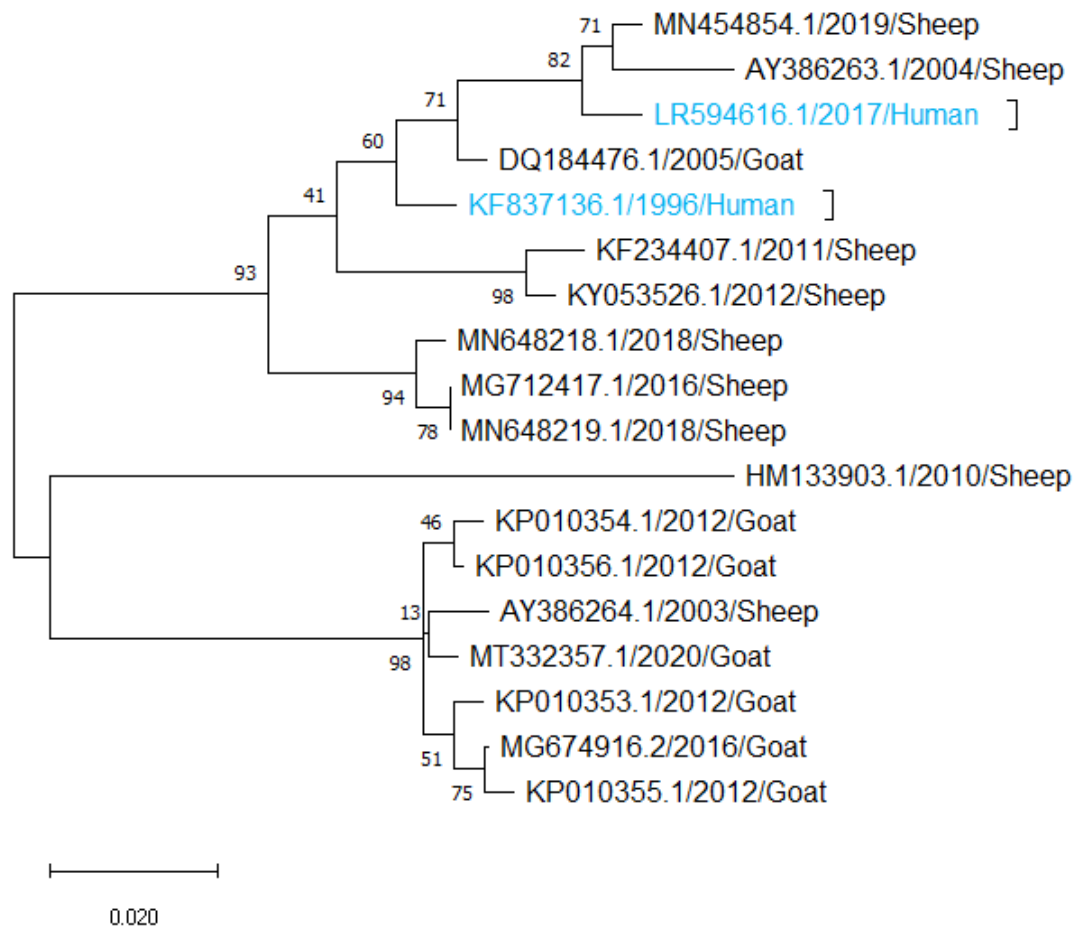


**Figure S.11: Phylogenetic analysis based on ORF120 nucleotide sequences.** Maximum likelihood method was used for analysis with a bootstrap test (1000 replicate). The tree is drawn to scale, with branch lengths in the same units as those of the evolutionary distances used to infer the phylogenetic tree. The human derived ORFV isolates are highlighted in blue.

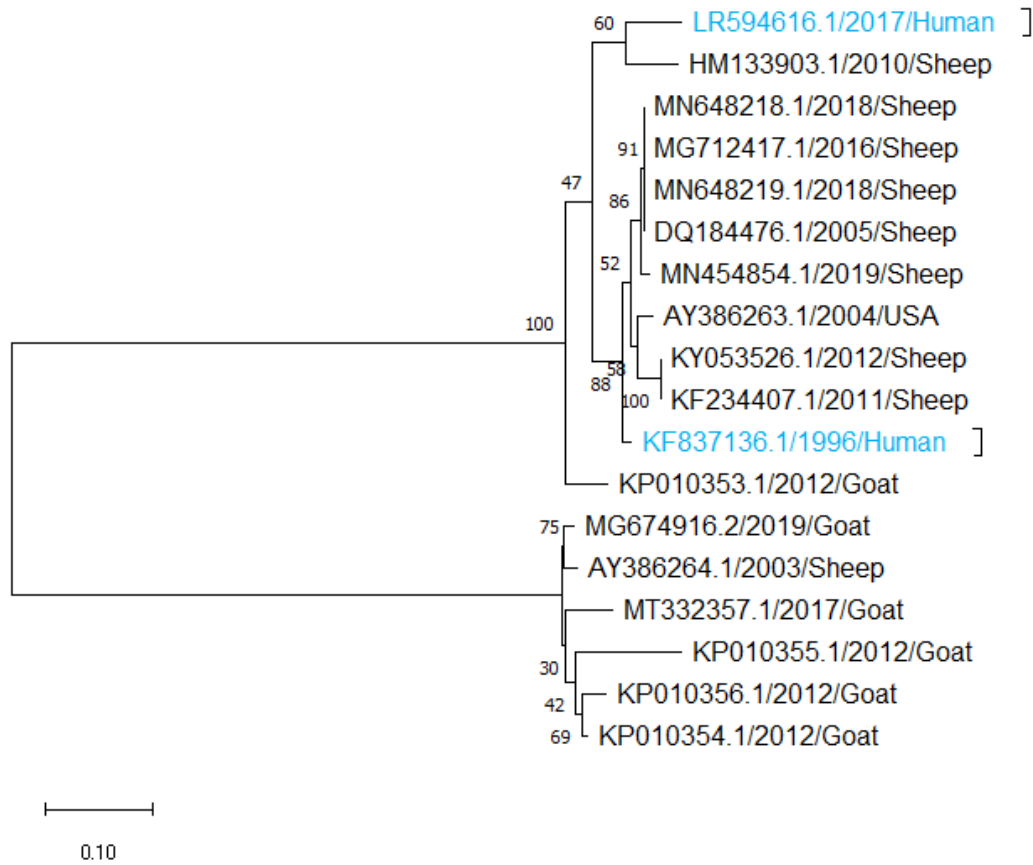


**Figure S.12: Phylogenetic analysis based on ORF132 nucleotide sequences.** Maximum likelihood method was used for analysis with a bootstrap test (1000 replicate). The tree is drawn to scale, with branch lengths in the same units as those of the evolutionary distances used to infer the phylogenetic tree. The human derived ORFV isolates are highlighted in blue.

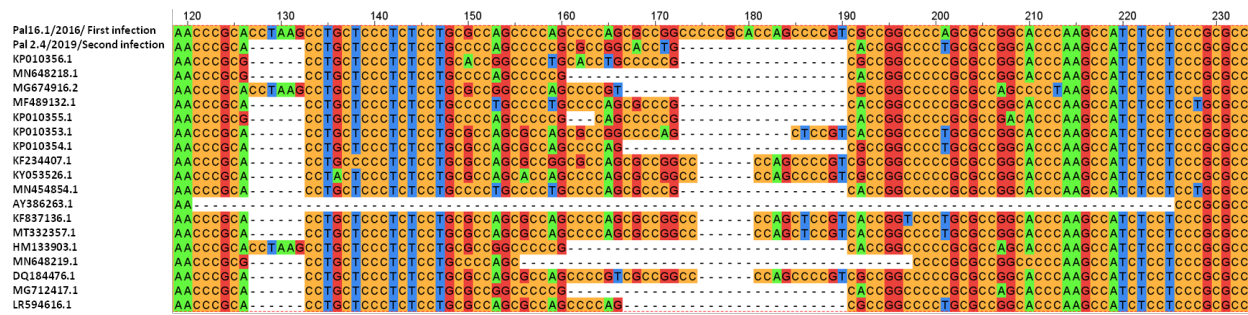


**Figure S.13: Divergence of F1L gene of ORFV in the 5'-terminal region.** Nucleotide sequence analysis of the F1L gene of ORFV isolates from the two infections and other sequences showed sequence heterogeneity (base pair variation and deletion) in the 5'- terminal regions.